bioRxiv preprint doi: https://doi.org/10.1101/2022.01.16.476523; this version posted January 17, 2022. The copyright holder for this preprint (which was not certified by peer review) is the author/funder, who has granted bioRxiv a license to display the preprint in perpetuity. It is made available under aCC-BY 4.0 International license.

Novel MBLs inhibitors screened from FDA-approved drug library restore the susceptibility of carbapenems to NDM-1-harbouring bacteria

Yan Guo[1#], Hongtao Liu[1#], Mengge Yang[1#], Rui Ding[1], Yawen Gao[2], Xiaodi Niu[2], Xuming Deng[1], Jianfeng Wang[1*], Haihua Feng[1*], Jiazhang Qiu[1*]

[1] Key Laboratory of Zoonosis, Ministry of Education, College of Veterinary Medicine, Jilin University, Changchun, Jilin 130062, China

[2] College of Food Science and Engineering, Jilin University, Changchun, Jilin 130062, China

[#] These authors contributed equally to this work.

[*] Corresponding authors: Jiazhang Qiu, qiujz@jlu.edu.cn; Haihua Feng, fhh70@163.com; Jianfeng Wang, wjf927@jlu.edu.cn.

bioRxiv preprint doi: https://doi.org/10.1101/2022.01.16.476523; this version posted January 17, 2022. The copyright holder for this preprint (which was not certified by peer review) is the author/funder, who has granted bioRxiv a license to display the preprint in perpetuity. It is made available under aCC-BY 4.0 International license.

Abstract

The production of metallo-β-lactamases (MBLs) is one of the major mechanisms adopted by bacterial pathogens to resist carbapenems. One promising strategy to overcome MBLs-mediated carbapenems resistance is to develop effective inhibitors. Repurposing approved drugs to restore the efficacy of carbapenems represents an efficient and cost-effective approach to fight infections caused by carbapenem resistant pathogens. Here, twelve FDA-approved compounds were screened to neutralize the ability of NDM-1. Among these compounds, dexrazoxane, embelin, candesartan cilexetil (CAN) and nordihydroguaiaretic acid (NDGA) were further demonstrated to inhibit all tested MBLs, and showed an *in vitro* synergistic bactericidal effect with meropenem against MBLs-producing bacteria. Mechanistic studies revealed that dexrazoxane, embelin and CAN are metal ion chelating agents, while the inhibition of NDM-1 by NDGA involves its direct binding with the active region of NDM-1. Furthermore, dexrazoxane, embelin and CAN and NDGA dramatically rescued the treatment efficacy of meropenem in three infection models. Our observations indicated that dexrazoxane, embelin, CAN and NDGA are promising carbapenem adjuvants against MBLs-positive carbapenem resistant bacterial pathogens.

Keywords: Carbapenems, Carbapenem-resistant Gram-negative bacteria, Metallo-β-lactamase, FDA-approved drug library, Drug repurposing

bioRxiv preprint doi: https://doi.org/10.1101/2022.01.16.476523; this version posted January 17, 2022. The copyright holder for this preprint (which was not certified by peer review) is the author/funder, who has granted bioRxiv a license to display the preprint in perpetuity. It is made available under aCC-BY 4.0 International license.

Introduction

The overuse and misuse of antibiotics has led to the rapid development and dissemination of antimicrobial resistance (AMR), which is a serious threat to public health worldwide. Currently, few therapeutic options are available for the treatment of infections caused by multi-drug resistant (MDR) bacteria, especially "ESKAPE" pathogens (*Enterococcus faecium*, *Staphylococcus aureus*, *Klebsiella pneumoniae*, *Acinetobacter baumannii*, *Pseudomonas aeruginosa* and *Enterobacter spp* [1]. It was estimated that AMR will result in 10 million patient deaths per year by 2050 unless active and effective actions are mounted [2].

Carbapenems are β-lactam antibiotics that are commonly used as last-resort drugs for the treatment of serious MDR gram-negative bacterial infections [3]. In the past two decades, the clinical consumption of carbapenems has increased dramatically, which is inevitably accompanied by the emergence and prevalence of carbapenem-resistant strains [4]. In particular, carbapenem-resistant *Enterobacteriaceae* (CRE), which has become a global public threat [5]. The production of an inactivating enzyme, carbapenemase, is the major resistance mechanism of *Enterobacteriaceae* to carbapenems [6]. The large numbers of carbapenemases are divided into three major categories according to their amino acid sequences. Classes A and D carbapenemases (e.g. KPC and OXA-48) are serine β-lactamases (SBLs), which utilize an active serine residue to covalently attack the β-lactam ring [7]. Class B carbapenemases represented by NDM, IMP and VIM are metallo-β-lactamases (MBLs), which require zinc ions for the activation of a water nucleophile to hydrolyse the ring [7, 8]. The global spread of

bioRxiv preprint doi: https://doi.org/10.1101/2022.01.16.476523; this version posted January 17, 2022. The copyright holder for this preprint (which was not certified by peer review) is the author/funder, who has granted bioRxiv a license to display the preprint in perpetuity. It is made available under aCC-BY 4.0 International license.

MBLs is particularly problematic and has aroused significant concerns due to their ability to inactivate almost all clinically approved β-lactams except for aztreonam [9]. In addition, MBLs have great potential for horizontal gene transfer between various bacterial species through MBLs-bearing plasmids [8]. The SENTRY antimicrobial surveillance program reported that the detection of MBL genes in CRE isolates were rapidly increased from 4.3% during 2007-2009 to 12.7% during 2014-2016, among which NDM was the most predominant type of MBLs, accounting for approximately 10% of the CRE isolates [10].

Carbapenem-resistant bacteria including *Acinetobacter baumannii*, *Pseudomonas aeruginosa* and *Enterobacteriaceae* were listed by the World Health Organization (WHO) in 2019 as the priority pathogens required for new treatment [10, 11]. Compared with the development of novel antibiotics, the discovery of carbapenemase inhibitors represents a fast and cost-effective alternative approach to restore the susceptibility of bacteria to carbapenems [12]. The advantages were further strengthened by advances in rapid detection technologies, enabling fast and accurate detection of carbapenemase genes [13-15]. Indeed, this strategy has yielded the successful development of SBL inhibitors. For example, vaborbactam was approved in 2017 for clinical use in combination with meropenem to overcome carbapenem resistance mediated by the expression of SBLs [16]. However, to date, no MBL inhibitors have been approved for clinical use to date.

Here, we screened 1515 FDA-approved drugs through the nitrocefin hydrolysis assay, resulting in the identification of 12 compounds that are capable of inhibiting

bioRxiv preprint doi: https://doi.org/10.1101/2022.01.16.476523; this version posted January 17, 2022. The copyright holder for this preprint (which was not certified by peer review) is the author/funder, who has granted bioRxiv a license to display the preprint in perpetuity. It is made available under aCC-BY 4.0 International license.

NDM-1 activity. We further confirmed that dexrazoxane, embelin, candesartan cilexetil (CAN) and nordihydroguaiaretic acid (NDGA) showed significant synergistic antibacterial effects when used in combination with meropenem against NDM-1 positive bacterial strains. In addition to affecting NDM-1, these compounds also exhibit broad inhibitory effects on other major types of MBLs, including IMP and VIM. Further mechanistic studies revealed that dexrazoxane, embelin and CAN are metal ion chelators, while the inhibition of MBLs by NDGA involves NDGA binding to the active region of NDM-1, preventing the binding of NDM-1 to its substrate and thereby inhibiting the activity of NDM-1. Finally, the combination therapy of the compounds with meropenem restored the treatment efficacy of meropenem in mice infected with NDM-1 harbouring *E. coli* isolates. Taken together, our study provides additional options for the treatment of infections caused by MBLs-positive bacterial pathogens.

Materials and Methods

Bacterial strains, plasmids, culture methods and reagents

The bacterial strains, plasmids and primers used in this study are listed in Supplementary **Table S1**, **Table S2** and **Table S3**, respectively. All bacterial strains were grown on Luria-Bertani (LB) plates or in LB broth. All NDM-1-positive strains were originated from our previous studies [17]. *E. cloacae* 20710 and *E. cloacae* 20712 were provided by Dr. Yonghong Xiao at Zhejiang University [18]. *A. baumannii* 21 was provided by Dr. Zhimin Guo at the First Hospital of Jilin University.

The full gene sequences of $bla_{\text{IMP-1}}$, $bla_{\text{VIM-1}}$, $bla_{\text{KPC-2}}$ and $bla_{\text{OXA-48}}$ were synthesized by GeneScript (Nanjing, China) and were inserted into pET28a or

bioRxiv preprint doi: https://doi.org/10.1101/2022.01.16.476523; this version posted January 17, 2022. The copyright holder for this preprint (which was not certified by peer review) is the author/funder, who has granted bioRxiv a license to display the preprint in perpetuity. It is made available under aCC-BY 4.0 International license.

pETSUMO for protein expression.

The FDA-approved drug library was purchased from ApexBio Technology (Cat#L1021, Houston, TX, USA). Dexrazoxane, embelin, CAN and NDGA were dissolved in DMSO (Sigma-Aldrich, St. Louis, MO, USA). Meropenem, amoxicillin, ciprofloxacin, imipenem, erythromycin, chloramphenicol, tetracycline and gentamicin were obtained from Dalian Meilun Biotechnology Co., Ltd. (Dalian, China).

Protein expression and purification

Plasmids derived from pET28a or pETSUMO for protein production were transformed into *E. coli* strain BL21 (DE3). Transformed *E. coli* was inoculated into LB broth containing kanamycin (final concentration of 30 μg/mL) and grown to an OD_{600nm} of 0.8 at 37 ºC, followed by induction with isopropyl-β-d-thiogalactoside (IPTG) overnight at 18 ºC. Cells were collected by centrifugation and lysed by a homogenizer (JN-mini, JNBIO, Guangzhou, China). Lysed samples were centrifuged at 12, 000 rpm for 20 min. NDM-1 and its mutant proteins, IMP-1, VIM-1, KPC-2 and OXA-48 were purified by nickel affinity chromatography. After washing with lysis buffer, proteins were eluted with 250 mM imidazole and dialyzed twice in a buffer containing 20 mM Tris-HCl (pH 7.5), 150 mM NaCl, 10% glycerol and 1 mM dithiothreitol (DTT). Protein concentrations were measured by the Bradford Protein Assay (Bio-Rad).

Nitrocefin hydrolysis assays

Nitrocefin hydrolysis assays were determined as described previously [17] in the presence of the indicated concentrations (from 0 to 64 μg/mL) of different compounds.

bioRxiv preprint doi: https://doi.org/10.1101/2022.01.16.476523; this version posted January 17, 2022. The copyright holder for this preprint (which was not certified by peer review) is the author/funder, who has granted bioRxiv a license to display the preprint in perpetuity. It is made available under aCC-BY 4.0 International license.

The results were read in 96-well plates at 37 ºC using a microplate reader at 492 nm (SYNERGY H1, BioTek). The inhibitory effects of the identified active compound on other carbapenemases (NDM-3, NDM-9, IMP-1, VIM-1, KPC-2 and OXA-48) were tested as described above using nitrocefin as the substrate.

Determination of the MIC and FICI

MIC values were determined according to the broth microdilution guidelines of the Clinical and Laboratory Standards Institute (CLSI). After the tested strains were diluted with LB to a final concentration of 5×10^5 CFUs/mL, various concentrations of meropenem (0-256 μg/mL) and increasing concentrations of inhibitors (0-64 μg/mL) were added to the sterile 96-well plate, and further incubated for 18-24 h at 37 ºC. The lowest concentration with no visible growth was considered as the MIC value. The synergistic effect of antibiotics and inhibitors was assessed by determining the fractional inhibitory concentration (FIC) index values according to the formula: FICI = (MIC of inhibitors in combination/MIC of inhibitors) + (MIC of antibiotics in combination/MIC of antibiotics).

Combined disc tests

Overnight bacterial culture was diluted with LB broth to an OD_{600nm} of 0.1. 200 μL of the bacterial suspension was plated on the LB plates. 10 μL of each inhibitor was added to the discs that containing 10 μg meropenem (Oxoid Ltd. Basingstoke, United Kingdom). The discs were placed in the center of the LB plates and incubated at 37 ºC for 24 h. Then, the inhibition zone of different treatments was measured and recorded.

Time-dependent killing

bioRxiv preprint doi: https://doi.org/10.1101/2022.01.16.476523; this version posted January 17, 2022. The copyright holder for this preprint (which was not certified by peer review) is the author/funder, who has granted bioRxiv a license to display the preprint in perpetuity. It is made available under aCC-BY 4.0 International license.

To determine the *in vitro* time-dependent killing of NDM-1 producing bacteria by meropenem, bacterial strains were incubated with inhibitors (32 or 64 μg/mL), meropenem (2 or 8 μg/mL), or inhibitors (32 or 64 μg/mL) in combination with meropenem (2 or 8 μg/mL) at 37 ºC. At the indicated time points, samples of different treatments were collected, diluted and plated on LB plates. The CFU values were calculated after incubation overnight at 37 ºC.

Inductively coupled plasma-mass spectrometry (ICP-MS)

ICP-MS was performed as described earlier [19] to investigate the potential ability of the identified NDM-1 inhibitors to chelate zinc ions. Briefly, in order to remove the contained metals, freshly purified NDM-1 protein was exchanged in ICP-MS buffer (20 mM HEPES, 100 mM NaCl, pH 7.5) overnight at 4 ºC in a 15 kDa cutoff dialysis tubing. The NDM-1 concentration was adjusted to 5 mg/mL prior to mixing with different concentrations of inhibitors and incubating for 3 h at room temperature with shaking. The NDM-1-inhibitor samples were then dialyzed overnight at 4 ºC with ICP-MS buffer by the 12-14 kDa cutoff D-tube dialyzer mini (EMD Biosciences) microdialysis cassettes. The samples were diluted to 1 mg/mL with ICP-MS buffer and then diluted 40-fold with an internal standard containing 10 ng/mL Sc^{45} and 1% nitric acid. Then, the samples were analysed by ICP-MS (XSERIES 2, Thermo Fisher Scientific).

Metal ions restoration assays

NDM-1 was pretreated with various concentrations of the inhibitors at 37 ºC for 10 min, followed by the addition of metal salts ($ZnSO_4$, $MgSO_4$ and $CaCl_2$) and nitrocefin to a final volume of 200 μL and an incubation for 30 min at 37 ºC. Then, the

bioRxiv preprint doi: https://doi.org/10.1101/2022.01.16.476523; this version posted January 17, 2022. The copyright holder for this preprint (which was not certified by peer review) is the author/funder, who has granted bioRxiv a license to display the preprint in perpetuity. It is made available under aCC-BY 4.0 International license.

177 absorbance at 492 nm of each sample was measured to calculate the percent residual
178 activity.

179 **Molecular dynamics simulation**

180 Molecular dynamics simulations of the NDGA-NDM-1 complexes were
181 performed using the Gromacs 4.5.2 software package [20] based on the GRO MOS96
182 54a7 force field and TIP3P water model. The molecular mechanics/Poisson-Boltzmann
183 surface area (MM-PBSA) method was used to calculate the binding free energy after
184 simulation as described previously [17].

185 **Secondary structure determination of NDM-1 by circular dichroism (CD)**
186 **spectroscopy**

187 The CD spectrum of NDM-1 was analysed using a CD spectrophotometer (MOS-
188 500; Bio-Logic, France) [21]. 200 μg of NDM-1 was incubated with 32 μg/mL of each
189 inhibitor. Then, the secondary structure of NDM-1 (0.2 mg/mL) was determined at
190 room temperature using a quartz cuvette with an optical distance of 1 mm. The scan
191 wavelength range was 190 to 250 nm with a resolution of 0.2 nm and a bandwidth of 1
192 nm. The BeStSel web server was used to analyse the secondary structure measurements
193 of each sample.

194 **Plasmid stability**

195 NDM-1-positive *E. coli*, *K. pneumoniae* and *A. baumannii* strains were grown in
196 LB broth overnight with constant shaking in the presence or absence of inhibitors (32
197 μg/mL). Bacteria were diluted and plated on blank LB plates or LB plates containing
198 30 μg/mL of kanamycin and incubated at 37 ºC for CFU determination.

bioRxiv preprint doi: https://doi.org/10.1101/2022.01.16.476523; this version posted January 17, 2022. The copyright holder for this preprint (which was not certified by peer review) is the author/funder, who has granted bioRxiv a license to display the preprint in perpetuity. It is made available under aCC-BY 4.0 International license.

199 **Antibodies and Immunoblotting**

200 Polyclonal antibodies against NDM-1 were produced by immunization of mice
201 with recombinant His_6-NDM-1 (AbMax Biotechnology Co., Ltd., Beijing, China).
202 NDM-1-positive bacterial strains were cultured in the presence of increasing
203 concentrations of inhibitors at 37 ºC for 12 h. Bacterial cultures were centrifuged at
204 12,000 rpm for 5 min, resuspended in 1× loading buffer and subjected to SDS-PAGE.
205 The proteins were transferred to polyvinylidene fluoride (PVDF) membranes followed
206 by a blocking step using 5% nonfat milk. Membranes were incubated with primary
207 antibody (1: 2000) for 2 h and secondary antibody for 1 h at room temperature. The
208 expression of NDM-1 was detected by the Odyssey® CLx Imaging System (Li-Cor).

209 **Ethics statement**

210 All animal studies were conducted according to the experimental practices and
211 standards approved by the Institutional Animal Care and Use Committee of Jilin
212 University (ALKT202102001). The laboratory animal usage license number is SYXK-
213 2021-0001, as certified by the Department of Science & Technology of Jilin Province.
214 All surgery was performed under sodium pentobarbital anesthesia, and every effort was
215 made to minimize suffering.

216 **Mouse infection models**

217 Female BALB/c mice (6-8 weeks old, approximately 20 g) were used in this study.
218 Mice were injected intraperitoneally with *E. coli* ZJ487 at a dose of 2×10^8 CFUs for
219 survival experiments, intramuscularly injected at a dose of 2×10^7 CFUs for bacterial
220 burden experiments on thigh muscles or inoculated in the left nare (5×10^7 CFUs) to

bioRxiv preprint doi: https://doi.org/10.1101/2022.01.16.476523; this version posted January 17, 2022. The copyright holder for this preprint (which was not certified by peer review) is the author/funder, who has granted bioRxiv a license to display the preprint in perpetuity. It is made available under aCC-BY 4.0 International license.

generate a pneumonia model. For all experiments, after the bacterial challenge, mice were given subcutaneous injections of DMSO, meropenem (10 mg/kg), inhibitors (80 mg/kg), or a combination of meropenem (10 mg/kg) with inhibitors (80 mg/kg) every 12 h. The infected mice were monitored until 96 h post infection for survival analysis. For the thigh muscle and pneumonia models, mice were euthanized 72 h post infection and the thigh muscles and lungs were harvested. Organs were placed into 1 mL of sterilized PBS and homogenized. Then, the suspension was diluted with PBS and plated on an LB plate for CFU enumeration. In addition, lungs were placed into 4% formalin, stained with haematoxylin and eosin and scanned with a digital slide scanner (Pannoramic MIDI, 3DHISTECH Ltd).

Statistical analysis

The statistical analysis was performed by GraphPad Prism 5 and SPSS software. All the data are presented as the mean ± SD. For *in vitro* studies, the statistical analysis was calculated by the unpaired two tailed Student's *t*-tests; for *in vivo* experiments, the statistical significance was determined using the log-rank (Mantel-Cox) test (survival rates) and Mann-Whitney U test (tissue bacterial load). $P < 0.05$ was considered as significant difference, with * indicating $P < 0.05$ and ** indicating $P < 0.01$.

Results

Four new NDM-1 inhibitors restore the sensitivity of NDM-1-positive bacterial strains to meropenem

bioRxiv preprint doi: https://doi.org/10.1101/2022.01.16.476523; this version posted January 17, 2022. The copyright holder for this preprint (which was not certified by peer review) is the author/funder, who has granted bioRxiv a license to display the preprint in perpetuity. It is made available under aCC-BY 4.0 International license.

To probe for the potential application of an existing drug as an NDM-1 inhibitor, we screened a commercially available FDA-approved drug library comprising 1515 compounds for their ability to inhibit the hydrolysis of nitrocefin to chromogenic cephalosporin by purified NDM-1 enzyme. The initial screening resulted in the identification of 12 compounds that were capable of inhibiting the enzymatic activity of NDM-1, with IC_{50} values ranging from 1.77 μg/mL to 10.71 μg/mL (**Figure 1** and **Table S4**). None of the compounds showed antibacterial activity against the tested gram-negative bacterial strains, as evident by all the MICs being no lower than 128 μg/mL. We further determined the potential synergistic effects of the compounds with carbapenems. Only four compounds (dexrazoxane, embelin, CAN and NDGA) significantly restored the susceptibility of meropenem against engineered *E. coli* strains expressing NDM-1 (BL21-pET28a-SP-NDM-1) or carbapenem-resistant bacterial isolates harbouring bla_{NDM-1}, as indicated by an FICI less than 0.5 (**Figure 2A** and **Tables S5-S8**). In addition, the combined disk tests also showed significant synergy between meropenem and the inhibitors. Compared to the disks containing meropenem alone, the diameter of the inhibition zone was significantly larger in disks containing both meropenem and each tested inhibitor (**Figure 2B** and **Figure2- figure supplement 1**). Moreover, the time-dependent killing curves were determined to investigate their synergistic bactericidal activity. We found that the combinations led to almost complete bacterial killing within 4 to 10 h for engineered *E. coli* BL21 expressing NDM-1 as well as the clinical *E. coli* isolate ZJ487 (**Figure 2C**). Thus, our results identified that dexrazoxane, embelin, CAN and NDGA represent effective NDM-1 inhibitors

bioRxiv preprint doi: https://doi.org/10.1101/2022.01.16.476523; this version posted January 17, 2022. The copyright holder for this preprint (which was not certified by peer review) is the author/funder, who has granted bioRxiv a license to display the preprint in perpetuity. It is made available under aCC-BY 4.0 International license.

displaying synergistic antibacterial activity against NDM-1-positive bacteria with meropenem.

Dexrazoxane, embelin, CAN and NDGA are broad-spectrum MBLs inhibitors

To verify the specificity of the NDM-1 inhibitors identified from the FDA-approved drug library, we purified a series of carbapenemases and tested their enzymatic activity in the presence of dexrazoxane, embelin, CAN and NDGA. Not surprisingly, all the inhibitors displayed potent inhibitory effects on the NDM-3 and NDM-9, the NDM-1 variants that have only a single amino acid mutation (**Figure 3A-B**). The inhibitors also showed increased antibacterial activity of meropenem against clinical isolates expressing NDM-9 (**Tables S5-S8**). Furthermore, the ability of two other major types of MBLs, IMP-1 and VIM-1, to hydrolyse nitrocefin was significantly suppressed by these compounds (**Figure 3C-D**). Therefore, dexrazoxane, embelin, CAN and NDGA could act as broad-spectrum MBLs inhibitors. Indeed, they were able to rescue the susceptibility of meropenem against carbapenem-resistant *E. cloacae* isolates mediated by the production of VIM-1 (**Tables S5-S8**). Surprisingly, embelin, CAN and NDGA but not dexrazoxane also exhibited varying degrees of inhibition of class A (KPC-2) and class D (OXA-48) carbapenemases (**Figure 3- figure supplement 1A-B**). Taken together, these results indicated that dexrazoxane, embelin, CAN and NDGA are broad-spectrum MBLs inhibitors.

Dexrazoxane, embelin and CAN act as metal ion chelators to inhibit the activity of NDM-1

bioRxiv preprint doi: https://doi.org/10.1101/2022.01.16.476523; this version posted January 17, 2022. The copyright holder for this preprint (which was not certified by peer review) is the author/funder, who has granted bioRxiv a license to display the preprint in perpetuity. It is made available under aCC-BY 4.0 International license.

To gain insights into the mechanisms adopted by the inhibitors to neutralize NDM-1, we first added excessive zinc ions in the nitrocefin hydrolysis reactions in the presence or absence of inhibitors. The efficacy of dexrazoxane, embelin and CAN in suppressing NDM-1 enzymatic activity was significantly reduced with the addition of 500 μM of $ZnSO_4$ (**Figure 4A-B**). Additionally, supplementation with other divalent metal ions (magnesium and calcium ions) in the reaction resulted in a similar restoration of NDM-1 activity (**Figure 4C-D**). Therefore, the inhibition of NDM-1 by dexrazoxane, embelin and CAN may be involved in a metal depletion mechanism. Indeed, after incubation of NDM-1 with 8 or 32 μg/mL of dexrazoxane, embelin and CAN, the zinc ion concentrations associated with NDM-1 were significantly reduced as determined by ICP-MS (**Figure 4E**). Taken together, dexrazoxane, embelin and CAN function as metal chelating agents to suppress the enzymatic activity of MBLs. In contrast, we did not observe either restoration of hydrolysing activity by supplementation with metal ions or the loss of zinc ions in NDM-1 inactivated by NDGA (**Figure 4A-E**), suggesting a different inhibitory mechanism employed by NDGA.

A direct engagement of NDGA inhibits NDM-1 activity

To further clarify the mechanism of NDGA on the inhibition of NDM-1, we carried out molecular dynamics simulations. A complex MD simulation of the NDM-1-NDGA complex was aimed to explore the binding mode (**Figure 5A**). The root mean square deviation (RMSD) of the complex fluctuated between 0.3 and 0.35 nm after 20 ns, which indicated that the last 80 ns period of the simulation was suitable for the subsequent analysis (**Figure 5B**). Energy decomposition analysis confirmed that the

bioRxiv preprint doi: https://doi.org/10.1101/2022.01.16.476523; this version posted January 17, 2022. The copyright holder for this preprint (which was not certified by peer review) is the author/funder, who has granted bioRxiv a license to display the preprint in perpetuity. It is made available under aCC-BY 4.0 International license.

side chains of IIe35, Cys208, Lys211, Asp212, Ala215, Met248 and His250 could bind to NDGA via van der Waals interactions (**Figure 5C**). Moreover, the distance between different residues of NDM-1 and NDGA was analysed. The IIe35, Lys211 and His250 in the NDM-1-binding region are closer to NDGA than other residues (distance < 0.4 nm) (**Figure 5D**). The simulated residues (IIe35, Lys211 and His250) that had the highest binding energy were selected for site-directed mutagenesis. Single mutations of IIe35, Lys211 and His250 into alanine did not affect the enzymatic activity of NDM-1. However, the inhibitory effect of NDGA on NDM-1_{I35A} and NDM-1_{K211A} but not NDM-1_{H250A} was significantly reduced (**Figure 5E**). Collectively, we speculated that NDGA could bind IIe35 and Lys211 to inhibit the activity of NDM-1.

Alteration of the secondary structure of NDM-1 by dexrazoxane, embelin, CAN and NDGA

In addition to the aforementioned mechanisms, we further detected whether these inhibitors affected the secondary structure of NDM-1 by CD spectroscopy. In the absence of inhibitors, the NDM-1 contains 52.5% α-helix and 22.0% turn conformations. However, following treatment of NDM-1 with 32 μg/mL of the inhibitors, the percentage of α-helix conformation was reduced to 0%, 18.8%, 0% and 17.2% for dexrazoxane, embelin, CAN and NDGA, respectively (**Figure 6A**). The percentage of turn conformation was increased to 76.7%, 54.3%, 70.3% and 46.1%, respectively. Additionally, NDGA-treated NDM-1 maintained a highly consistent conformational composition with untreated NDM-1, and only the proportion of different conformations is changed, while the conformation of dexrazoxane, embelin or

bioRxiv preprint doi: https://doi.org/10.1101/2022.01.16.476523; this version posted January 17, 2022. The copyright holder for this preprint (which was not certified by peer review) is the author/funder, who has granted bioRxiv a license to display the preprint in perpetuity. It is made available under aCC-BY 4.0 International license.

CAN-treated NDM-1 (including heat inactivated NDM-1) changed dramatically compared with that of untreated NDM-1 (**Figure 6A**). With the addition of inhibitors, the negative ellipticity of the CD spectrum of NDM-1 decreased, and the negative peak at 222 nm was shifted to higher wavenumbers accompanied by a shortened amplitude (**Figure 6B**). Such conformational changes may be attributed to the direct interaction between inhibitors and NDM-1 or the indirect influence of zinc ions depletion within NDM-1 caused by the inhibitors. However, the currently available structural biology data did not clearly clarify the importance of zinc ion on the structural stability of NDM-1. Thus, our results indicated that treatment with dexrazoxane, embelin, CAN and NDGA measurably altered the secondary structure of NDM-1.

Dexrazoxane and embelin reduce the protein stability of NDM-1

In addition to the direct inhibition of NDM-1, we further assessed whether these compounds affect the production of NDM-1. Bacterial strains harbouring plasmid-borne $bla_{\text{NDM-1}}$ were treated with increasing concentrations of inhibitors, and the total cell lysates were subsequently subjected to immunoblotting to determine the protein level of NDM-1. We found that the amount of NDM-1 was remarkably reduced in response to 32 μg/mL of dexrazoxane and embelin but not NDGA or CAN (**Figure 7A** and **Figure 7- figure supplement 1A**). The reduced level of NDM-1 did not result from the loss of plasmid stability by the effect of dexrazoxane and embelin (**Figure 7- figure supplement 2**). It was previously reported earlier that zinc ion depletion could accelerate the degradation of MBLs in bacteria [22]. Hence, the decreased amount of NDM-1 in the tested bacterial isolates could be the consequence of metal ion removal

bioRxiv preprint doi: https://doi.org/10.1101/2022.01.16.476523; this version posted January 17, 2022. The copyright holder for this preprint (which was not certified by peer review) is the author/funder, who has granted bioRxiv a license to display the preprint in perpetuity. It is made available under aCC-BY 4.0 International license.

by dexrazoxane and embelin. Indeed, we observed a restored amount of NDM-1 in the sample with an addition of excessive zinc ions in bacteria treated with 32 μg/mL of dexrazoxane and embelin (**Figure 7B** and **Figure 7- figure supplement 1B**). CAN, another metal ion chelator, was not observed detected to reduce the amount of NDM-1 at the tested concentration, probably due to its weaker chelating capability or relatively poor permeability to bacterial cells, which failed to efficiently remove zinc ions associated with NDM-1. Taken together, our data suggested that deletion of zinc ions by dexrazoxane and embelin could induce the degradation of NDM-1.

Dexrazoxane, embelin, CAN and NDGA restore meropenem activity *in vivo*

Given the potent inhibition of dexrazoxane, embelin, CAN and NDGA on the enzymatic activity of NDM-1, as well as their excellent *in vitro* synergistic bactericidal activity against NDM-1 producing bacterial pathogens when used in combination with meropenem, we further investigated the potential application of these inhibitors to overcome carbapenem resistance *in vivo* and restore the treatment efficacy of meropenem in the clinical settings. We established three mouse infection models to assess the *in vivo* therapeutic effects of the combined therapy. In the lethal systemic infection model, all mice infected with *E. coli* ZJ487 treated with PBS or meropenem monotherapy died within 36 h post-infection. However, the combined therapy of meropenem with the inhibitors resulted in 33.33%, 50%, 66.67% and 33.33% survival for dexrazoxane, NDGA, embelin and CAN, respectively (**Figure 8A**). Surprisingly, embelin alone can also increase the survival rate of mice to 33%, which may be due to its unexplored pharmacological actions on either mammalian hosts or bacteria cells.

bioRxiv preprint doi: https://doi.org/10.1101/2022.01.16.476523; this version posted January 17, 2022. The copyright holder for this preprint (which was not certified by peer review) is the author/funder, who has granted bioRxiv a license to display the preprint in perpetuity. It is made available under aCC-BY 4.0 International license.

The therapeutic advantages of the combined therapy were also supported by the mouse thigh muscle infection model. The bacterial load was reduced significantly in infected mice treated with meropenem and the individual NDM-1 inhibitors (**Figure 8- figure supplement 1A**). Moreover, we tested the treatment efficacy of the combination therapy in a mouse pneumonia infection model. Co-therapy of mice with meropenem and NDM-1 inhibitors resulted in strikingly lower bacterial counts in the lungs (**Figure 8- figure supplement 1B**) and as well as the marked remission of pulmonary inflammation as evidenced by less inflammatory factor infiltration in the alveolar space (**Figure 8B**). Together, these observations confirmed the potential utilization of dexrazoxane, embelin, CAN and NDGA to rescue carbapenem activity *in vivo* against infections caused by NDM-1 producing bacterial pathogens.

Discussion

Carbapenems are still the last-resort antibiotics to control serious infectious diseases caused by MDR gram-negative bacterial pathogens. However, the development of carbapenem resistance mediated by carbapenemase has greatly limited the clinical use of carbapenems. Therefore, it is urgent to develop novel treatment strategies to address infections caused by carbapenem resistant bacteria. In recent decades, many scientific groups have concentrated on the identification of novel effective β-lactamase inhibitors, and fortunately resulting in significant progress [23]. The most striking achievements are the discovery of diazabicyclooctanones (DBOs), non-β-lactam β-lactamase inhibitors [24]. Recently, two DBOs (avibactam and

bioRxiv preprint doi: https://doi.org/10.1101/2022.01.16.476523; this version posted January 17, 2022. The copyright holder for this preprint (which was not certified by peer review) is the author/funder, who has granted bioRxiv a license to display the preprint in perpetuity. It is made available under aCC-BY 4.0 International license.

395 relebactam) have been approved for clinical use in combination with β-lactams such as
396 ceftazidime, imipenem and cilastatin [25-27]. Moreover, two novel DBO-type
397 inhibitors, zidebactam and nacubactam, which have high affinity for penicillin-binding
398 protein 2 and potent inhibition of β-lactamase, are under investigation in clinical trials
399 combined with β-lactams [28-30]. In addition to DBOs, another type of non-β-lactam
400 β-lactamase inhibitor, vaborbactam, which contains a cyclic boronic acid
401 pharmacophore, was available on the market and used in conjunction with meropenem
402 [31]. Obviously, the clinical application of DBOs and vaborbactam expanded the
403 therapeutic options for lethal diseases by gram-negative bacteria. However, both DBOs
404 and vaborbactam are narrow-spectrum inhibitors and are only active towards SBLs but
405 not MBLs [24, 32]. Hence, the identification of inhibitors against MBLs is highly
406 urgent and represents the major challenge in the field of β-lactamase inhibitor
407 development. A great number of compounds such as thiols, thioesters,
408 azolylthioacetamide, carboxylic acids, cyclic boronates and aspergillomarasmine A
409 showed activity to inhibit MBLs by diverse mechanisms [19, 33]. Despite of the
410 worldwide academic efforts, no MBLs inhibitors are close to clinical use.

411 Compared to the *de novo* development of an entirely new drug for a specific
412 disease, drug repurposing, which aims to identify novel applications for existing drugs,
413 has gained increasing interest during the last decade [34, 35]. This strategy exhibits
414 significant advantages since the repurposed drugs already have pharmacokinetic and
415 safety assessment data, which can greatly reduce the timeline and cost of development.
416 Here we employed the repurposing approach and found four NDM-1 inhibitors from

bioRxiv preprint doi: https://doi.org/10.1101/2022.01.16.476523; this version posted January 17, 2022. The copyright holder for this preprint (which was not certified by peer review) is the author/funder, who has granted bioRxiv a license to display the preprint in perpetuity. It is made available under aCC-BY 4.0 International license.

the FDA-approved drugs. Dexrazoxane is used mainly as an anti-tumor adjuvant drug to alleviate the cardiotoxicity induced by anthracycline [36]; NDGA is an antioxidant applied mostly in the food industry [37]; embelin, a natural compound isolated from *Embeliaribes*, is a well-known antagonist for X-linked inhibitor of apoptosis protein (XIAP) used for the treatment of various cancers [38]; CAN is a potent blocker of angiotens in II receptor approved to treat hypertension in adults [39]. These four inhibitors showed broad-spectrum inhibitory effects on MBLs either by chelating zinc ions (dexrazoxane, embelin and CAN) or by directly engaging MBLs (NDGA). When used in combination with meropenem, these inhibitors displayed potent synergistic bactericidal effects on MBLs-producing bacteria *in vitro*. In addition, combined therapy with meropenem and inhibitors also exhibits synergistic treatment advantages against infections induced by bacteria expressing NDM-1.

It was noted that an earlier study also reported embelin as an NDM-1 inhibitor from an enzymatic-based screening of naturally occurring chemicals [40]. Here, we further demonstrated that embelin functions as a potent chelating agent to directly deplete zinc ions from NDM-1, and further clarified its potential application in combined therapy with meropenem against MBLs-harbouring bacteria in various animal infection models.

Conclusion

Our data demonstrated that the FDA-approved dexrazoxane, embelin, CAN and NDGA possess excellent synergistic activity with meropenem against carbapenem-resistant bacteria mediated by MBLs both *in vitro* and *in vivo*. Our observations together

bioRxiv preprint doi: https://doi.org/10.1101/2022.01.16.476523; this version posted January 17, 2022. The copyright holder for this preprint (which was not certified by peer review) is the author/funder, who has granted bioRxiv a license to display the preprint in perpetuity. It is made available under aCC-BY 4.0 International license.

439 with the established safety assessments indicate the great potential of repurposing these
440 drugs as antibiotic adjuvants to fight lethal infections caused by MBLs-producing
441 bacterial pathogens.

442

443 **Acknowledgements**

444 The authors thank Professor Yonghong Xiao (Zhejiang University, China) for
445 strains *E. cloacae* 20710 and 20712, and thank Dr. Zhimin Guo (the First Hospital of
446 Jilin University, China) for *A. baumannii* 21. This work was supported by the National
447 Key Research and Development Program of China (2021YFD1801000), the National
448 Natural Science Foundation of China (grant nos. 81861138046 and 32172912).

449

450 **Conflicts of interest**

451 All authors declare no conflict of interest.

452
453

bioRxiv preprint doi: https://doi.org/10.1101/2022.01.16.476523; this version posted January 17, 2022. The copyright holder for this preprint (which was not certified by peer review) is the author/funder, who has granted bioRxiv a license to display the preprint in perpetuity. It is made available under aCC-BY 4.0 International license.

References

1. De Oliveira DMP, Forde BM, Kidd TJ, Harris PNA, Schembri MA, Beatson SA, et al. Antimicrobial Resistance in ESKAPE Pathogens. Clin Microbiol Rev. 2020; 33.

2. de Kraker ME, Stewardson AJ, Harbarth S. Will 10 Million People Die a Year due to Antimicrobial Resistance by 2050? PLoS Med. 2016; 13: e1002184.

3. McKenna M. Antibiotic resistance: the last resort. Nature. 2013; 499: 394-6.

4. Zequinao T, Telles JP, Gasparetto J, Tuon FF. Carbapenem stewardship with ertapenem and antimicrobial resistance-a scoping review. Rev Soc Bras Med Trop. 2020; 53: e20200413.

5. Patel G, Bonomo RA. "Stormy waters ahead": global emergence of carbapenemases. Front Microbiol. 2013; 4: 48.

6. Nordmann P, Poirel L. Epidemiology and Diagnostics of Carbapenem Resistance in Gram-negative Bacteria. Clin Infect Dis. 2019; 69: S521-S8.

7. Queenan AM, Bush K. Carbapenemases: the versatile beta-lactamases. Clin Microbiol Rev. 2007; 20: 440-58, table of contents.

8. Yong D, Toleman MA, Giske CG, Cho HS, Sundman K, Lee K, et al. Characterization of a new metallo-beta-lactamase gene, bla(NDM-1), and a novel erythromycin esterase gene carried on a unique genetic structure in Klebsiella pneumoniae sequence type 14 from India. Antimicrob Agents Chemother. 2009; 53: 5046-54.

9. van Duin D, Doi Y. The global epidemiology of carbapenemase-producing Enterobacteriaceae. Virulence. 2017; 8: 460-9.

bioRxiv preprint doi: https://doi.org/10.1101/2022.01.16.476523; this version posted January 17, 2022. The copyright holder for this preprint (which was not certified by peer review) is the author/funder, who has granted bioRxiv a license to display the preprint in perpetuity. It is made available under aCC-BY 4.0 International license.

476 10. Castanheira M, Deshpande LM, Mendes RE, Canton R, Sader HS, Jones RN.
477 Variations in the Occurrence of Resistance Phenotypes and Carbapenemase Genes
478 Among Enterobacteriaceae Isolates in 20 Years of the SENTRY Antimicrobial
479 Surveillance Program. Open Forum Infect Dis. 2019; 6: S23-S33.
480 11. WHO. Global Priority List of Antibiotic-Resistant Bacteria to Guide Research,
481 Discovery, and Development of New Antibiotics. . 2020.
482 12. Bush K, Bradford PA. Interplay between beta-lactamases and new beta-lactamase
483 inhibitors. Nat Rev Microbiol. 2019; 17: 295-306.
484 13. Pasteran F, Gonzalez LJ, Albornoz E, Bahr G, Vila AJ, Corso A. Triton Hodge Test:
485 Improved Protocol for Modified Hodge Test for Enhanced Detection of NDM and Other
486 Carbapenemase Producers. J Clin Microbiol. 2016; 54: 640-9.
487 14. Kumar N, Singh VA, Beniwal V, Pottathil S. Modified Carba NP Test: Simple and
488 rapid method to differentiate KPC- and MBL-producing Klebsiella species. J Clin Lab
489 Anal. 2018; 32: e22448.
490 15. Howard JC, Creighton J, Ikram R, Werno AM. Comparison of the performance of
491 three variations of the Carbapenem Inactivation Method (CIM, modified CIM [mCIM]
492 and in-house method (iCIM)) for the detection of carbapenemase-producing
493 Enterobacterales and non-fermenters. J Glob Antimicrob Resist. 2020; 21: 78-82.
494 16. Zhanel GG, Lawrence CK, Adam H, Schweizer F, Zelenitsky S, Zhanel M, et al.
495 Imipenem-Relebactam and Meropenem-Vaborbactam: Two Novel Carbapenem-beta-
496 Lactamase Inhibitor Combinations. Drugs. 2018; 78: 65-98.
497 17. Liu S, Zhang J, Zhou Y, Hu N, Li J, Wang Y, et al. Pterostilbene restores

bioRxiv preprint doi: https://doi.org/10.1101/2022.01.16.476523; this version posted January 17, 2022. The copyright holder for this preprint (which was not certified by peer review) is the author/funder, who has granted bioRxiv a license to display the preprint in perpetuity. It is made available under aCC-BY 4.0 International license.

carbapenem susceptibility in New Delhi metallo-beta-lactamase-producing isolates by inhibiting the activity of New Delhi metallo-beta-lactamases. Br J Pharmacol. 2019; 176: 4548-57.

18. Zhou K, Yu X, Zhou Y, Song J, Ji Y, Shen P, et al. Detection of an In104-like integron carrying a blaIMP-34 gene in Enterobacter cloacae isolates co-producing IMP-34 and VIM-1. J Antimicrob Chemother. 2019; 74: 2812-4.

19. King AM, Reid-Yu SA, Wang W, King DT, De Pascale G, Strynadka NC, et al. Aspergillomarasmine A overcomes metallo-beta-lactamase antibiotic resistance. Nature. 2014; 510: 503-6.

20. Hess B, Kutzner C, van der Spoel D, Lindahl E. GROMACS 4: Algorithms for Highly Efficient, Load-Balanced, and Scalable Molecular Simulation. Journal of chemical theory and computation. 2008; 4: 435-47.

21. Zhou Y, Guo Y, Wen Z, Ci X, Xia L, Wang Y, et al. Isoalantolactone Enhances the Antimicrobial Activity of Penicillin G against Staphylococcus aureus by Inactivating beta-lactamase during Protein Translation. Pathogens. 2020; 9.

22. Sychantha D, Rotondo CM, Tehrani K, Martin NI, Wright GD. Aspergillomarasmine A inhibits metallo-beta-lactamases by selectively sequestering Zn(2). J Biol Chem. 2021; 297: 100918.

23. Tooke CL, Hinchliffe P, Bragginton EC, Colenso CK, Hirvonen VHA, Takebayashi Y, et al. beta-Lactamases and beta-Lactamase Inhibitors in the 21st Century. J Mol Biol. 2019; 431: 3472-500.

24. de Sousa Coelho F, Mainardi JL. The multiple benefits of second-generation beta-

bioRxiv preprint doi: https://doi.org/10.1101/2022.01.16.476523; this version posted January 17, 2022. The copyright holder for this preprint (which was not certified by peer review) is the author/funder, who has granted bioRxiv a license to display the preprint in perpetuity. It is made available under aCC-BY 4.0 International license.

520 lactamase inhibitors in treatment of multidrug-resistant bacteria. Infect Dis Now. 2021;
521 51: 510-7.
522 25. Giri P, Patel H, Srinivas NR. Review of Clinical Pharmacokinetics of Avibactam,
523 A Newly Approved non-beta lactam beta-lactamase Inhibitor Drug, In Combination
524 Use With Ceftazidime. Drug Res (Stuttg). 2019; 69: 245-55.
525 26. Campanella TA, Gallagher JC. A Clinical Review and Critical Evaluation of
526 Imipenem-Relebactam: Evidence to Date. Infect Drug Resist. 2020; 13: 4297-308.
527 27. McCarthy MW. Clinical Pharmacokinetics and Pharmacodynamics of Imipenem-
528 Cilastatin/Relebactam Combination Therapy. Clin Pharmacokinet. 2020; 59: 567-73.
529 28. Moya B, Barcelo IM, Bhagwat S, Patel M, Bou G, Papp-Wallace KM, et al. WCK
530 5107 (Zidebactam) and WCK 5153 Are Novel Inhibitors of PBP2 Showing Potent
531 "beta-Lactam Enhancer" Activity against Pseudomonas aeruginosa, Including
532 Multidrug-Resistant Metallo-beta-Lactamase-Producing High-Risk Clones.
533 Antimicrob Agents Chemother. 2017; 61.
534 29. Livermore DM, Mushtaq S, Warner M, Vickers A, Woodford N. In vitro activity of
535 cefepime/zidebactam (WCK 5222) against Gram-negative bacteria. J Antimicrob
536 Chemother. 2017; 72: 1373-85.
537 30. Mallalieu NL, Winter E, Fettner S, Patel K, Zwanziger E, Attley G, et al. Safety
538 and Pharmacokinetic Characterization of Nacubactam, a Novel beta-Lactamase
539 Inhibitor, Alone and in Combination with Meropenem, in Healthy Volunteers.
540 Antimicrob Agents Chemother. 2020; 64.
541 31. Wu G, Cheon E. Meropenem-vaborbactam for the treatment of complicated urinary

bioRxiv preprint doi: https://doi.org/10.1101/2022.01.16.476523; this version posted January 17, 2022. The copyright holder for this preprint (which was not certified by peer review) is the author/funder, who has granted bioRxiv a license to display the preprint in perpetuity. It is made available under aCC-BY 4.0 International license.

542 tract infections including acute pyelonephritis. Expert Opin Pharmacother. 2018; 19:
543 1495-502.
544 32. Lomovskaya O, Sun D, Rubio-Aparicio D, Nelson K, Tsivkovski R, Griffith DC,
545 et al. Vaborbactam: Spectrum of Beta-Lactamase Inhibition and Impact of Resistance
546 Mechanisms on Activity in Enterobacteriaceae. Antimicrob Agents Chemother. 2017;
547 61.
548 33. Nagulapalli Venkata KC, Ellebrecht M, Tripathi SK. Efforts towards the inhibitor
549 design for New Delhi metallo-beta-lactamase (NDM-1). Eur J Med Chem. 2021; 225:
550 113747.
551 34. Pushpakom S, Iorio F, Eyers PA, Escott KJ, Hopper S, Wells A, et al. Drug
552 repurposing: progress, challenges and recommendations. Nat Rev Drug Discov. 2019;
553 18: 41-58.
554 35. Peyclit L, Baron SA, Rolain JM. Drug Repurposing to Fight Colistin and
555 Carbapenem-Resistant Bacteria. Front Cell Infect Microbiol. 2019; 9: 193.
556 36. Popelova O, Sterba M, Haskova P, Simunek T, Hroch M, Guncova I, et al.
557 Dexrazoxane-afforded protection against chronic anthracycline cardiotoxicity in vivo:
558 effective rescue of cardiomyocytes from apoptotic cell death. Br J Cancer. 2009; 101:
559 792-802.
560 37. Peralta I, Marrassini C, Filip R, Alonso MR, Anesini C. Food preservation by
561 Larrea divaricata extract: participation of polyphenols. Food Sci Nutr. 2018; 6: 1269-
562 75.
563 38. Sheng Z, Ge S, Gao M, Jian R, Chen X, Xu X, et al. Synthesis and Biological

bioRxiv preprint doi: https://doi.org/10.1101/2022.01.16.476523; this version posted January 17, 2022. The copyright holder for this preprint (which was not certified by peer review) is the author/funder, who has granted bioRxiv a license to display the preprint in perpetuity. It is made available under aCC-BY 4.0 International license.

564 Activity of Embelin and its Derivatives: An Overview. Mini Rev Med Chem. 2020; 20:
565 396-407.
566 39. Sawhney N, Patel MK, Schachter M, Hughes AD. Inhibition of proliferation by
567 heparin and expression of p53 in cultured human vascular smooth muscle cells. J Hum
568 Hypertens. 1997; 11: 611-4.
569 40. Ning NZ, Liu X, Chen F, Zhou P, Hu L, Huang J, et al. Embelin Restores
570 Carbapenem Efficacy against NDM-1-Positive Pathogens. Front Microbiol. 2018; 9:
571 71.
572
573

bioRxiv preprint doi: https://doi.org/10.1101/2022.01.16.476523; this version posted January 17, 2022. The copyright holder for this preprint (which was not certified by peer review) is the author/funder, who has granted bioRxiv a license to display the preprint in perpetuity. It is made available under aCC-BY 4.0 International license.

Tables

Table S1. Bacterial strains used in this study.

Bacterial Strains	Source	Identifier
E. coli ATCC25922	ATCC	25922
E. coli BL21 (DE3)	NEB	CAT#C2527I
E. coli pET28a-SP-NDM-1	This study	N/A
E. coli ZJ487 (NDM-1)	[1]	N/A
E. coli ZC-YN3 (NDM-1)	[1]	N/A
E. coli ZC-YN7 (NDM-9)	[1]	N/A
E. coli D3 (NDM-1)	[1]	N/A
E. coli E1 (NDM-1)	[1]	N/A
E. coli 2Z49 (NDM-5)	[1]	N/A
E. coli 2Z69 (NDM-5)	[1]	N/A
E. coli E4 (NDM-5)	[1]	N/A
E. coli E2 (NDM-9)	[1]	N/A
K. pneumoniae QD-KP1 (NDM-1)	[1]	N/A
K. pneumoniae QD-KP2 (NDM-1)	[1]	N/A
K. pneumoniae QD-KP3 (NDM-1)	[1]	N/A
E. cloacae 20710 (VIM-1)	[2]	N/A
E. cloacae 20712 (VIM-1)	[2]	N/A
A. baumanii 21	This study	N/A

References

1. Wang Y, Zhang R, Li J, Wu Z, Yin W, Schwarz S, et al. Comprehensive resistome analysis reveals the prevalence of NDM and MCR-1 in Chinese poultry production. Nat

bioRxiv preprint doi: https://doi.org/10.1101/2022.01.16.476523; this version posted January 17, 2022. The copyright holder for this preprint (which was not certified by peer review) is the author/funder, who has granted bioRxiv a license to display the preprint in perpetuity. It is made available under aCC-BY 4.0 International license.

579 Microbiol. 2017; 2: 16260.
580 2. Zhou K, Yu X, Zhou Y, Song J, Ji Y, Shen P, et al. Detection of an In104-like
581 integron carrying a blaIMP-34 gene in Enterobacter cloacae isolates co-producing IMP-
582 34 and VIM-1. J Antimicrob Chemother. 2019; 74: 2812-4.
583
584
585
586

bioRxiv preprint doi: https://doi.org/10.1101/2022.01.16.476523; this version posted January 17, 2022. The copyright holder for this preprint (which was not certified by peer review) is the author/funder, who has granted bioRxiv a license to display the preprint in perpetuity. It is made available under aCC-BY 4.0 International license.

587 **Table S2. Plasmids used in this study.**

Plasmids	Source	Identifier
pET28a	Novagen	CAT#69864
pETSUMO	Invitrogen	CAT#K300
pET28a-NDM-1	This study	N/A
pETSUMO-KPC-2	This study	N/A
pETSUMO-VIM-1	This study	N/A
pETSUMO-IMP-1	This study	N/A
pETSUMO-OXA-48	This study	N/A
pET28a-NDM-3	This study	N/A
pET28a-NDM-9	This study	N/A
pET28a-NDM-1$_{I35A}$	This study	N/A
pET28a-NDM-1$_{K211A}$	This study	N/A
pET28a-NDM-1$_{H250A}$	This study	N/A

588

589

bioRxiv preprint doi: https://doi.org/10.1101/2022.01.16.476523; this version posted January 17, 2022. The copyright holder for this preprint (which was not certified by peer review) is the author/funder, who has granted bioRxiv a license to display the preprint in perpetuity. It is made available under aCC-BY 4.0 International license.

590 **Table S3. Primers used in this study.**

Primers	Sequences[a, b]	Notes
YG601	ctgGGATCCTTGAATTCGCCCCATATT	$bla_{\text{sp-NDM-1}}$ BamHI-F
YG602	ctgGTCGACTCAGCGCAGCTTGTCGGCCAT	$bla_{\text{sp-NDM-1}}$ SalI-R
YG603	ctgGGATCCATGGAATTGCCCAAT	$bla_{\text{NDM-1}}$ BamHI-F
YG604	ctgGTCGACGACAAGCTGCGCTGA	$bla_{\text{NDM-1}}$ SalI-R
YG605	ctgGGATCCATGACCAACCTCGTCGCG	$bla_{\text{KPC-2}}$ BamHI-F
YG606	ctgGTCGACGCCCAATCCCTCGAG	$bla_{\text{KPC-2}}$ SalI-R
YG607	ctgGGATCCATGTTAAAAGTTATTAGTAGT	$bla_{\text{VIM-1}}$ BamHI-F
YG608	ctgCTCGAGCTACTCGGCGACTGAG	$bla_{\text{VIM-1}}$ XhoI-R
YG609	ctgGGATCCATGAGCAAACTGAGC	$bla_{\text{IMP-1}}$ BamHI-F
YG610	ctgGTCGACATGGTTGCTCGGTTTGCT	$bla_{\text{IMP-1}}$ SalI-R
YG611	ctgGGATCCTGGCAGGAAAACAAA	$bla_{\text{OXA-48}}$ BamHI-F
YG612	ctgGTCGACCGGAATAATTTTTTC	$bla_{\text{OXA-48}}$ SalI-R
YG613	CCGCCTGGACCAATGACCAGACC	$bla_{\text{NDM-3}}$ BamHI-F
YG614	GGTCTGGTCATTGGTCCAGGCGG	$bla_{\text{NDM-3}}$ SalI-R
YG615	CTTGCCCCGCAAAAGGGGATGGTTG	$bla_{\text{NDM-9}}$ BamHI-F
YG616	CAACCATCCCCTTTTGCGGGGCAAG	$bla_{\text{NDM-9}}$ SalI-R
YG617	GTGAAATCCGCCCGACGGCTGGCCAGCAAATG GAAA	$bla_{\text{NDM-1-}I35A}$-F
YG618	TTTCCATTTGCTGGCCAGCCGTCGGGCGGATTT CAC	$bla_{\text{NDM-1-}I35A}$-R
YG619	GGTGGCTGCCTGATCGCGGACAGCAAGGCCAA	$bla_{\text{NDM-1-}K211A}$-F
YG620	TTGGCCTTGCTGTCCGCGATCAGGCAGCCACC	$bla_{\text{NDM-1-}K211A}$-R
YG621	CATGATCGTGATGAGCGCTTCCGCCCCCGATAG C	$bla_{\text{NDM-1-}H250A}$-F
YG622	GCTATCGGGGGCGGAAGCGCTCATCACGATCA TG	$bla_{\text{NDM-1-}H250A}$-R

591 [a] Restriction enzyme sites are underlined.

592 [b] The mutated codons are underlined in red.

593

594

595

bioRxiv preprint doi: https://doi.org/10.1101/2022.01.16.476523; this version posted January 17, 2022. The copyright holder for this preprint (which was not certified by peer review) is the author/funder, who has granted bioRxiv a license to display the preprint in perpetuity. It is made available under aCC-BY 4.0 International license.

596 **Table S4. IC_{50} of the remaining active inhibitors on NDM-1.**

Number	Drug	Structure	IC_{50} (μg/mL)
1	Benserazide hydrochloride	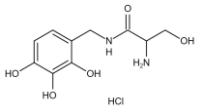	2.06
2	Broxyquinoline	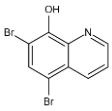	3.00
3	Gadodiamide	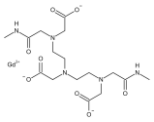	4.61
4	Sertaconazole nitrate	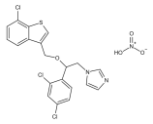	3.09
5	Dolutegravir Sodium	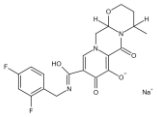	9.29
6	1, 4-Benzoquinone		3.79
7	Clotrimazole	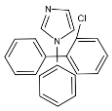	2.07
8	Fenticonazole nitrate	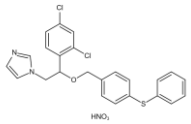	6.30

bioRxiv preprint doi: https://doi.org/10.1101/2022.01.16.476523; this version posted January 17, 2022. The copyright holder for this preprint (which was not certified by peer review) is the author/funder, who has granted bioRxiv a license to display the preprint in perpetuity. It is made available under aCC-BY 4.0 International license.

Table S5. Synergistic antibacterial effect of meropenem in combination with dexrazoxane on tested strains.

Species	Antibiotics	MIC (μg/mL)		FIC Index
		Alone	Combination	
***E. coli* ATCC 25922**	Meropenem	0.03±0.00	0.03±0.00	1.06±0.00
***E. coli* ZJ487 (NDM-1)**	Meropenem	32.00±0.00	1.00±0.00	**0.09±0.00**
	Amoxicillin	512.00±0.00	512.00±0.00	1.06±0.00
	Ciprofloxacin	512.00±0.00	341.33±120.68	0.73±0.24
	Imipenem	13.33±3.77	3.33±0.94	**0.31±0.00**
	Erythrocin	2.00±0.00	2.00±0.00	1.06±0.00
	Chloramphenicol	8.00±0.00	6.67±1.89	0.90±0.20
	Tetracycline	213.33±60.34	213.33±60.34	13.33±3.77
	Gentamicin	341.33±120.68	256.00±0.00	13.33±3.77
***E. coli* ZC-YN3 (NDM-1)**	Meropenem	21.33±7.54	2.67±0.94	**0.19±0.00**
***E. coli* ZC-YN7 (NDM-9)**	Meropenem	13.33±3.77	3.00±1.41	**0.27±0.06**
***E. coli* D3 (NDM-1)**	Meropenem	13.33±3.77	1.00±0.00	**0.15±0.03**
***E. coli* E1 (NDM-1)**	Meropenem	13.33±3.77	1.00±0.00	**0.15±0.03**
***E. coli* 2Z49 (NDM-5)**	Meropenem	32.00±0.00	4.00±0.00	**0.19±0.00**
***E. coli* 2Z69 (NDM-5)**	Meropenem	32.00±0.00	6.67±1.89	**0.27±0.06**
***E. coli* E4 (NDM-5)**	Meropenem	53.33±15.08	8.67±5.73	**0.24±0.1**
***E. coli* E2 (NDM-9)**	Meropenem	53.33±15.08	4.00±0.00	**0.15±0.03**
***K. pneumoniae* QD-KP1 (NDM-1)**	Meropenem	64.00±0.00	10.67±3.77	**0.23±0.06**
***K. pneumoniae* QD-KP2 (NDM-1)**	Meropenem	106.67±30.17	37.33±19.96	**0.40±0.12**
***K. pneumoniae* QD-KP3 (NDM-1)**	Meropenem	128.00±0.00	12.00±5.66	**0.10±0.02**
***E. coli* BL21 (pET28a-SP-NDM-1)**	Meropenem	128.00±0.00	5.33±1.89	**0.10±0.01**
***E. cloacae* 20710 (VIM-1)**	Meropenem	32.00±0.00	4.00±0.00	**0.19±0.00**
***E. cloacae* 20712 (VIM-1)**	Meropenem	32.00±0.00	5.33±1.89	**0.23±0.06**

Data are the mean ± SD from three independent experiments. Dexrazoxane, 64μg/mL.

bioRxiv preprint doi: https://doi.org/10.1101/2022.01.16.476523; this version posted January 17, 2022. The copyright holder for this preprint (which was not certified by peer review) is the author/funder, who has granted bioRxiv a license to display the preprint in perpetuity. It is made available under aCC-BY 4.0 International license.

Table S6. Synergistic antibacterial effect of meropenem in combination with NDGA on tested strains.

Species	Antibiotics	MIC (μg/mL)		FIC Index
		Alone	Combination	
***E. coli* ATCC 25922**	Meropenem	0.03±0.00	0.03±0.00	1.13±0.00
***E. coli* ZJ487 (NDM-1)**	Meropenem	32.00±0.00	1.00±0.00	**0.16±0.00**
	Amoxicillin	512.00±0.00	512.00±0.00	1.13±0.00
	Ciprofloxacin	512.00±0.00	426.67±120.68	0.96±0.24
	Imipenem	13.33±3.77	3.33±0.94	**0.38±0.00**
	Erythrocin	2.00±0.00	1.33±0.47	0.79±0.24
	Chloramphenicol	8.00±0.00	5.33±1.89	0.79±0.24
	Tetracycline	213.33±60.34	213.33±60.34	1.13±0.00
	Gentamicin	341.33±120.68	213.33±60.34	0.79±0.24
***E. coli* ZC-YN3 (NDM-1)**	Meropenem	21.33±7.54	2.67±0.94	**0.25±0.00**
***E. coli* ZC-YN7 (NDM-9)**	Meropenem	13.33±3.77	1.00±0.00	**0.21±0.03**
***E. coli* D3 (NDM-1)**	Meropenem	13.33±3.77	2.00±0.00	**0.29±0.06**
***E. coli* E1 (NDM-1)**	Meropenem	13.33±3.77	2.67±0.94	**0.33±0.03**
***E. coli* 2Z49 (NDM-5)**	Meropenem	32.00±0.00	8.00±0.00	**0.38±0.00**
***E. coli* 2Z69 (NDM-5)**	Meropenem	32.00±0.00	6.67±1.89	**0.33±0.06**
***E. coli* E4 (NDM-5)**	Meropenem	53.33±15.08	2.67±0.94	**0.19±0.10**
***E. coli* E2 (NDM-9)**	Meropenem	53.33±15.08	24.67±27.92	0.55±0.41
***K. pneumoniae* QD-KP1 (NDM-1)**	Meropenem	64.00±0.00	21.33±7.54	**0.46±0.12**
***K. pneumoniae* QD-KP2 (NDM-1)**	Meropenem	106.67±30.17	69.33±45.88	0.71±0.31
***K. pneumoniae* QD-KP3 (NDM-1)**	Meropenem	128.00±0.00	341.33±120.68	0.96±0.24
***E. coli* BL21 (pET28a-SP-NDM-1)**	Meropenem	128.00±0.00	26.67±7.54	**0.33±0.06**
***E. cloacae* 20710 (VIM-1)**	Meropenem	32.00±0.00	6.67±1.89	**0.33±0.06**
***E. cloacae* 20712 (VIM-1)**	Meropenem	32.00±0.00	8.00±0.00	**0.38±0.00**

Data are the mean ± SD from three independent experiments. NDGA, 32 μg/mL.

bioRxiv preprint doi: https://doi.org/10.1101/2022.01.16.476523; this version posted January 17, 2022. The copyright holder for this preprint (which was not certified by peer review) is the author/funder, who has granted bioRxiv a license to display the preprint in perpetuity. It is made available under aCC-BY 4.0 International license.

Table S7. Synergistic antibacterial effect of meropenem in combination with embelin on tested strains.

Species	Antibiotics	MIC (μg/mL)		FIC Index
		Alone	Combination	
***E. coli* ATCC 25922**	Meropenem	0.03±0.00	0.03±0.00	1.25±0.00
***E. coli* ZJ487 (NDM-1)**	Meropenem	32.00±0.00	0.03±0.00	**0.25±0.00**
	Amoxicillin	512.00±0.00	512.00±0.00	1.25±0.00
	Ciprofloxacin	512.00±0.00	426.67±120.68	1.08±0.24
	Imipenem	13.33±3.77	1.00±0.00	**0.33±0.03**
	Erythrocin	2.00±0.00	1.67±0.47	1.08±0.24
	Chloramphenicol	8.00±0.00	6.67±1.89	1.08±0.24
	Tetracycline	213.33±60.34	213.33±60.34	1.25±0.00
	Gentamicin	341.33±120.68	213.33±60.34	0.92±0.24
***E. coli* ZC-YN3 (NDM-1)**	Meropenem	21.33±7.54	0.25±0.00	**0.26±0.00**
***E. coli* ZC-YN7 (NDM-9)**	Meropenem	13.33±3.77	0.50±0.00	**0.29±0.01**
***E. coli* D3 (NDM-1)**	Meropenem	13.33±3.77	0.50±0.00	**0.29±0.01**
***E. coli* E1 (NDM-1)**	Meropenem	13.33±3.77	0.50±0.00	**0.29±0.01**
***E. coli* 2Z49 (NDM-5)**	Meropenem	32.00±0.00	0.33±0.12	**0.26±0.00**
***E. coli* 2Z69 (NDM-5)**	Meropenem	32.00±0.00	0.50±0.00	**0.27±0.00**
***E. coli* E4 (NDM-5)**	Meropenem	53.33±15.08	0.50±0.00	**0.26±0.00**
***E. coli* E2 (NDM-9)**	Meropenem	53.33±15.08	0.50±0.00	**0.26±0.00**
***K. pneumoniae* QD-KP1 (NDM-1)**	Meropenem	64.00±0.00	1.67±0.47	**0.28±0.01**
***K. pneumoniae* QD-KP2 (NDM-1)**	Meropenem	106.67±30.17	1.33±0.47	**0.27±0.01**
***K. pneumoniae* QD-KP3 (NDM-1)**	Meropenem	128.00±0.00	1.67±0.47	**0.28±0.01**
***E. coli* BL21 (pET28a-SP-NDM-1)**	Meropenem	128.00±0.00	0.50±0.00	**0.25±0.00**
***E. cloacae* 20710 (VIM-1)**	Meropenem	32.00±0.00	4.00±0.00	**0.26±0.00**
***E. cloacae* 20712 (VIM-1)**	Meropenem	32.00±0.00	0.25±0.00	**0.26±0.00**

Data are the mean ± SD from three independent experiments. Embelin, 32 μg/mL.

bioRxiv preprint doi: https://doi.org/10.1101/2022.01.16.476523; this version posted January 17, 2022. The copyright holder for this preprint (which was not certified by peer review) is the author/funder, who has granted bioRxiv a license to display the preprint in perpetuity. It is made available under aCC-BY 4.0 International license.

606 **Table S8. Synergistic antibacterial effect of meropenem in combination with CAN**
607 **on tested strains.**

Species	Antibiotics	MIC (μg/mL)		FIC Index
		Alone	Combination	
***E. coli* ATCC 25922**	Meropenem	0.03±0.00	0.03±0.00	1.06±0.00
	Meropenem	32.00±0.00	2.00±0.00	**0.13±0.00**
	Amoxicillin	512.00±0.00	512.00±0.00	1.06±0.00
	Ciprofloxacin	512.00±0.00	512.00±0.00	1.06±0.00
***E. coli* ZJ487 (NDM-1)**	Imipenem	13.33±3.77	1.33±0.47	**0.17±0.03**
	Erythrocin	2.00±0.00	1.67±0.47	0.90±0.24
	Chloramphenicol	8.00±0.00	8.00±0.00	1.06±0.00
	Tetracycline	213.33±60.34	170.67±60.34	0.90±0.24
	Gentamicin	341.33±120.68	341.33±120.68	1.06±0.00
***E. coli* ZC-YN3 (NDM-1)**	Meropenem	21.33±7.54	3.33±0.94	**0.23±0.06**
***E. coli* ZC-YN7 (NDM-9)**	Meropenem	13.33±3.77	3.33±0.94	**0.31±0.00**
***E. coli* D3 (NDM-1)**	Meropenem	13.33±3.77	1.67±0.47	**0.19±0.00**
***E. coli* E1 (NDM-1)**	Meropenem	13.33±3.77	2.33±1.25	**0.23±0.06**
***E. coli* 2Z49 (NDM-5)**	Meropenem	32.00±0.00	6.67±1.89	**0.27±0.06**
***E. coli* 2Z69 (NDM-5)**	Meropenem	32.00±0.00	5.33±1.89	**0.23±0.06**
***E. coli* E4 (NDM-5)**	Meropenem	53.33±15.08	10.67±3.77	**0.27±0.06**
***E. coli* E2 (NDM-9)**	Meropenem	53.33±15.08	13.33±13.20	**0.29±0.19**
***K. pneumoniae* QD-KP1 (NDM-1)**	Meropenem	64.00±0.00	16.00±0.00	**0.31±0.00**
***K. pneumoniae* QD-KP2 (NDM-1)**	Meropenem	106.67±30.17	8.00±0.00	**0.15±0.03**
***K. pneumoniae* QD-KP3 (NDM-1)**	Meropenem	128.00±0.00	256.00±0.00	0.73±0.24
***E. coli* BL21 (pET28a-SP-NDM-1)**	Meropenem	128.00±0.00	21.33±7.54	**0.23±0.06**
***E. cloacae* 20710 (VIM-1)**	Meropenem	32.00±0.00	10.67±3.77	**0.40±0.12**
***E. cloacae* 20712 (VIM-1)**	Meropenem	32.00±0.00	6.67±1.89	**0.27±0.06**

608 Data are the mean ± SD from three independent experiments. CAN, 64 μg/mL.

bioRxiv preprint doi: https://doi.org/10.1101/2022.01.16.476523; this version posted January 17, 2022. The copyright holder for this preprint (which was not certified by peer review) is the author/funder, who has granted bioRxiv a license to display the preprint in perpetuity. It is made available under aCC-BY 4.0 International license.

Figures

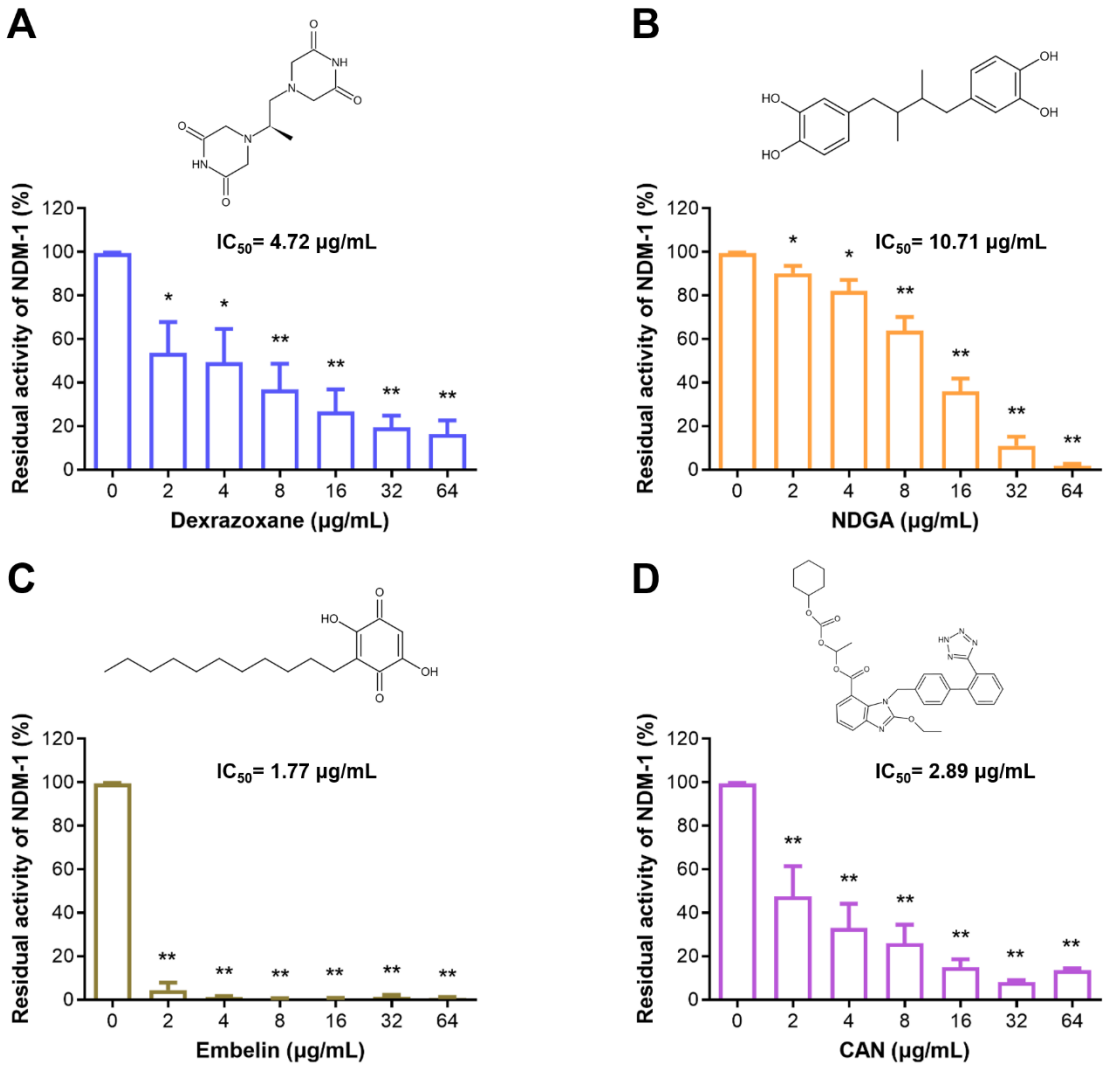

Figure 1. Four inhibitors were screened for their ability to inactivate NDM-1.

Inhibition of NDM-1 by dexrazoxane (**A**), NDGA (**B**), embelin (**C**) and CAN (**D**). The chemical structures of the inhibitors are shown in each panel. The positive control was performed in the presence of NDM-1 without inhibitors, while the negative control was carried out in the absence of enzyme. Percent residual activity of NDM-1 = A−A0/A100−A0 × 100%, where A represents the absorbance of samples at 492 nm, A0 and A100 represent 0% and 100% activity of enzyme as determined in the negative control and positive control, respectively. All the data represent the mean ± SD from

bioRxiv preprint doi: https://doi.org/10.1101/2022.01.16.476523; this version posted January 17, 2022. The copyright holder for this preprint (which was not certified by peer review) is the author/funder, who has granted bioRxiv a license to display the preprint in perpetuity. It is made available under aCC-BY 4.0 International license.

619 three independent experiments. * indicates $P < 0.05$ and ** indicates $P < 0.01$ by

620 Student's *t*-test.

621

bioRxiv preprint doi: https://doi.org/10.1101/2022.01.16.476523; this version posted January 17, 2022. The copyright holder for this preprint (which was not certified by peer review) is the author/funder, who has granted bioRxiv a license to display the preprint in perpetuity. It is made available under aCC-BY 4.0 International license.

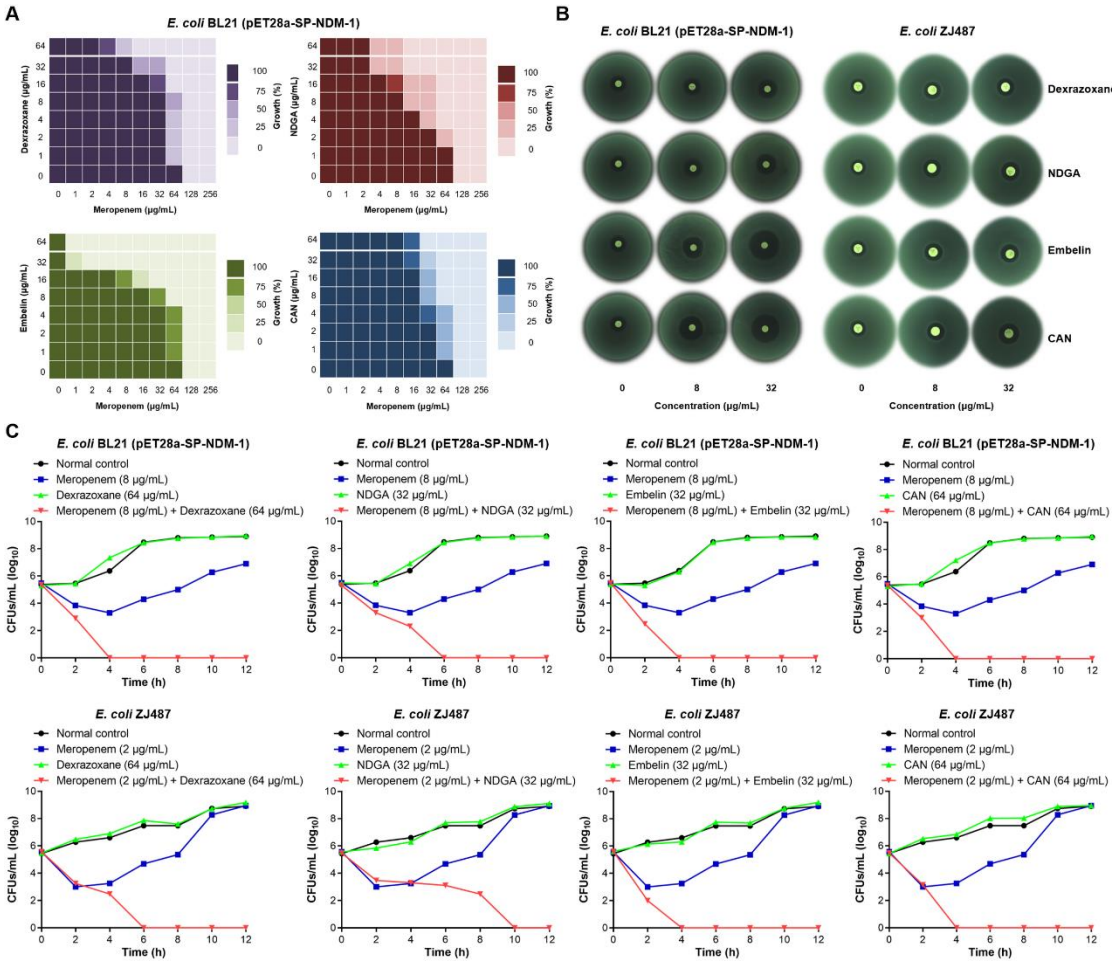

Figure 2. Dexrazoxane, NDGA, embelin and CAN rescue the antibacterial activity of meropenem *in vitro*.

(**A**) Microdilution checkerboard analysis showed the synergistic antibacterial effect of dexrazoxane, NDGA, embelin and CAN and meropenem against *E. coli* BL21 (pET28a-SP-NDM-1). (**B**) Zones of inhibition surrounding meropenem disks supplemented with increasing concentrations of dexrazoxane, NDGA, embelin and CAN for the NDM-1-positive strains. (**C**) Time-dependent killing by the combination of meropenem and dexrazoxane, NDGA, embelin or CAN against ZJ487 and *E. coli* BL21 (pET28a-SP-NDM-1). The data shown in panels **A, B** and **C** are one representative of three independent experiments.

bioRxiv preprint doi: https://doi.org/10.1101/2022.01.16.476523; this version posted January 17, 2022. The copyright holder for this preprint (which was not certified by peer review) is the author/funder, who has granted bioRxiv a license to display the preprint in perpetuity. It is made available under aCC-BY 4.0 International license.

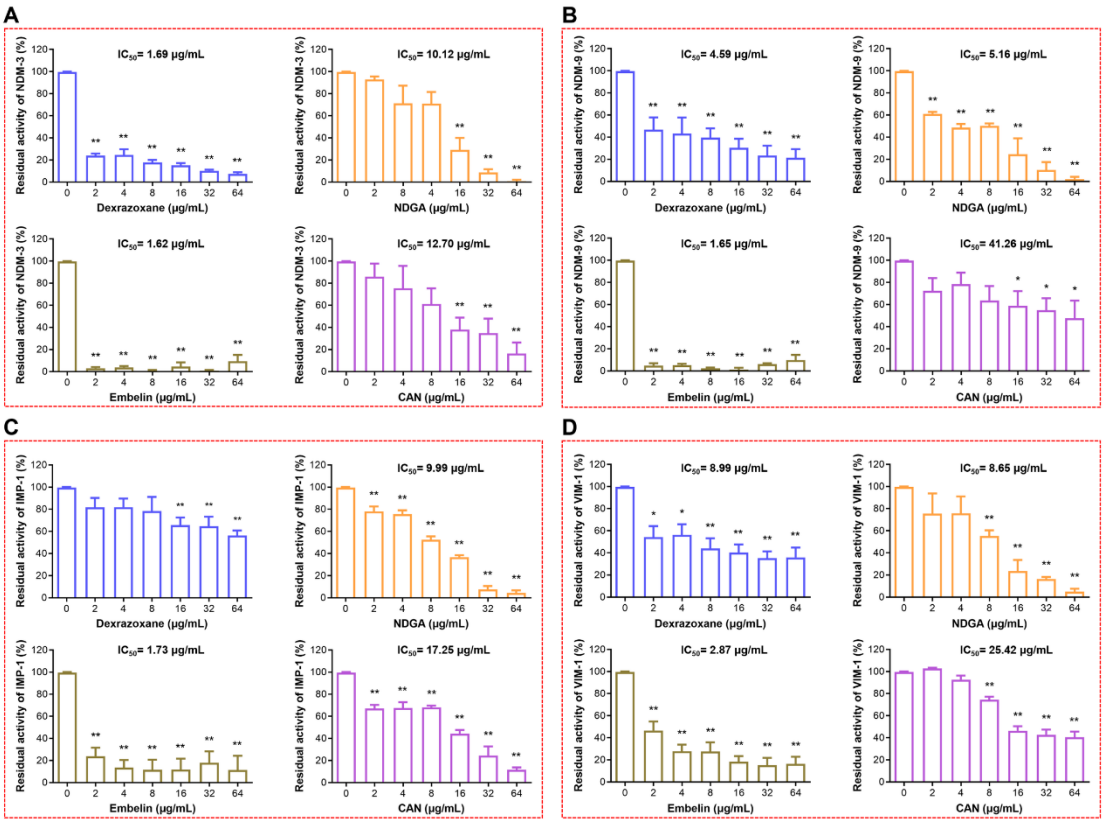

Figure 3. Dexrazoxane, NDGA, embelin and CAN suppress the activity of NDM-3, NDM-9, IMP-1 and VIM-1.

Following pre-incubation of dexrazoxane, NDGA, embelin and CAN with NDM-3 (**A**), NDM-9 (**B**), IMP-1 (**C**) and VIM-1 (**D**), the residual enzymatic activity of these proteins was determined as shown in Figure 1. The data shown are the mean ± SD from three independent experiments. * indicates $P < 0.05$ and ** indicates $P < 0.01$ by Student's *t*-test.

bioRxiv preprint doi: https://doi.org/10.1101/2022.01.16.476523; this version posted January 17, 2022. The copyright holder for this preprint (which was not certified by peer review) is the author/funder, who has granted bioRxiv a license to display the preprint in perpetuity. It is made available under aCC-BY 4.0 International license.

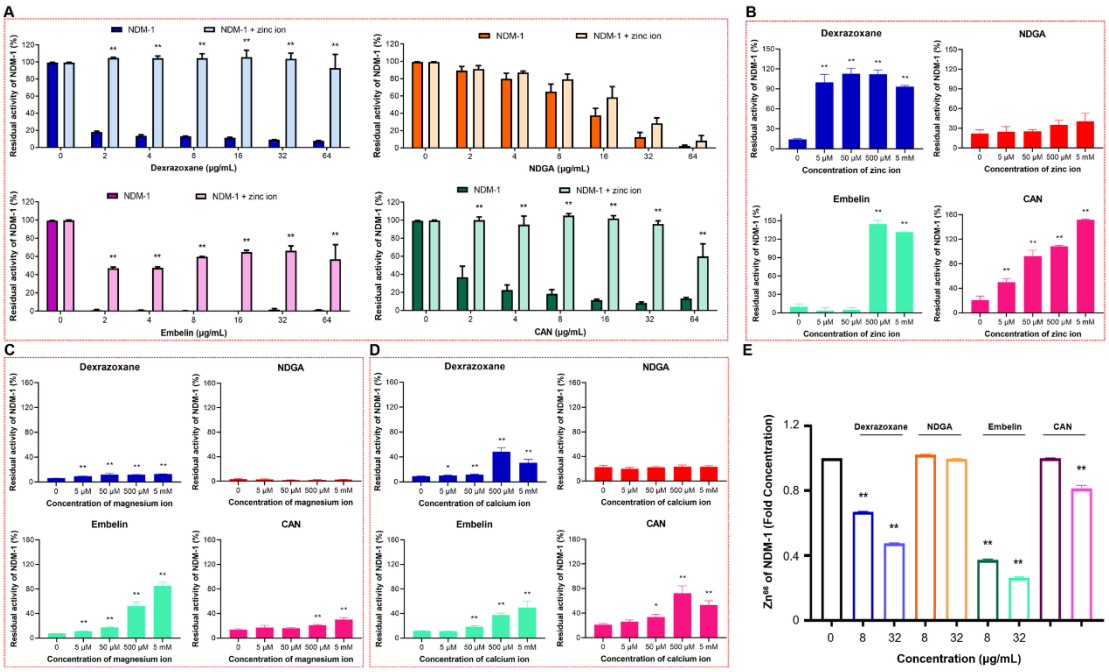

Figure 4. Dexrazoxane, embelin and CAN act as metal ion chelators to inhibit NDM-1 activity.

(**A**) Residual activity of NDM-1 after the addition of 500 μM zinc ions in the presence of increasing concentrations of dexrazoxane, NDGA, embelin and CAN. **(B-D)** Supplementation with increasing concentrations of zinc ions **(B)**, magnesium ions **(C)** and calcium ions **(D)** relieved the inhibition of NDM-1 mediated by dexrazoxane, embelin and CAN. (**E**) Zinc ion depletion by dexrazoxane, embelin and CAN as determined by ICP-MS. The vertical coordinate represents the fold concentration of free Zn^{66} in NDM-1. The data shown are the mean ± SD from three independent experiments. * indicates $P < 0.05$ and ** indicates $P < 0.01$ by Student's *t*-test.

bioRxiv preprint doi: https://doi.org/10.1101/2022.01.16.476523; this version posted January 17, 2022. The copyright holder for this preprint (which was not certified by peer review) is the author/funder, who has granted bioRxiv a license to display the preprint in perpetuity. It is made available under aCC-BY 4.0 International license.

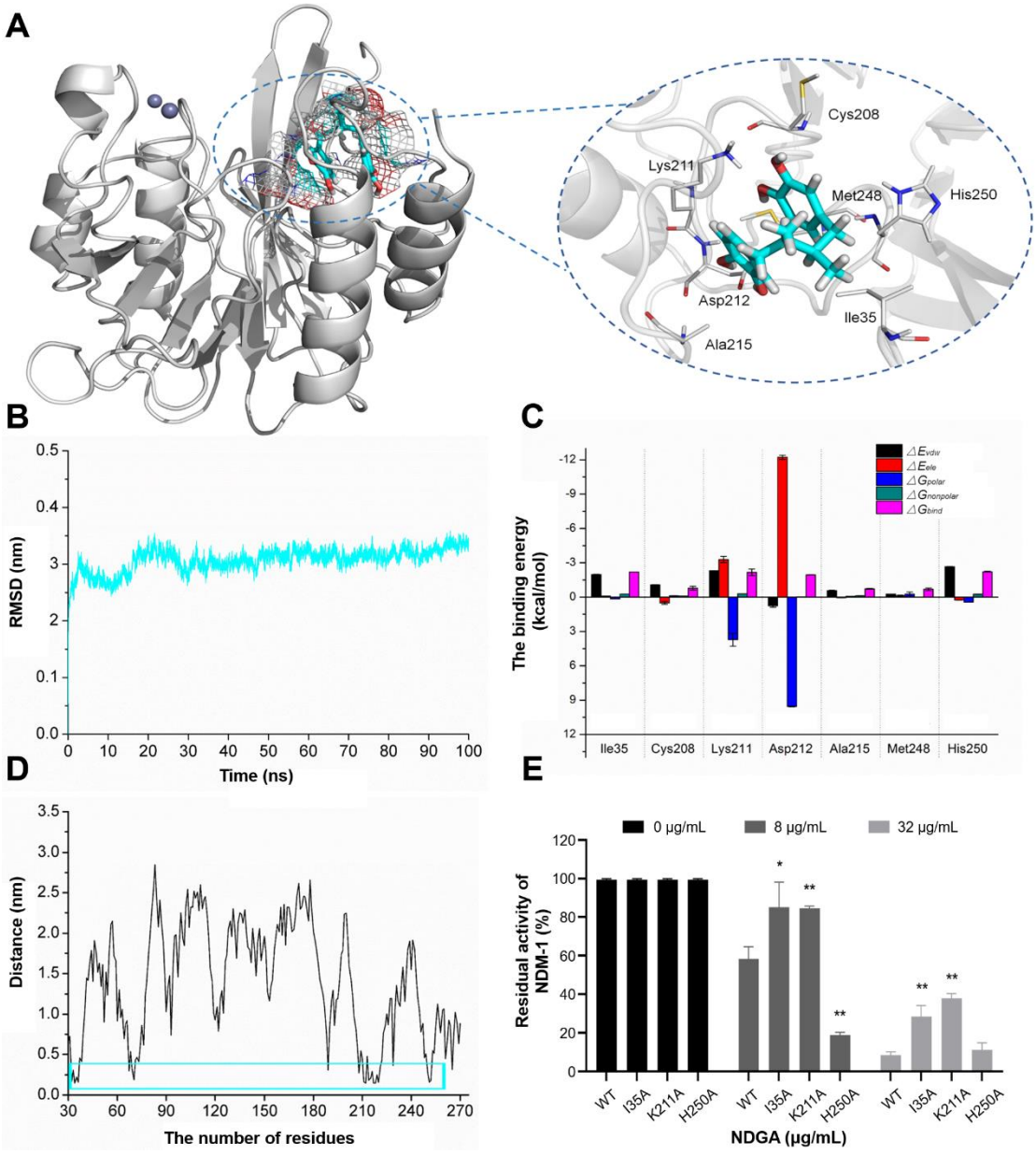

Figure 5. Direct engagement of NDGA with NDM-1.

(**A**) The three-dimensional structure determination of NDM-1 with the NDGA complex via a molecular modelling method. The purple spheres represent zinc ions. (**B**) The RMSD values of the NDM-1-NDGA complex. (**C**) Decomposition of the binding energy on a per-residue basis in the binding sites of the NDM-1-NDGA complex. (**D**) Analysis of the distance between all residues of NDM-1 and NDGA. (**E**) Residual activity of NDM-1 and its mutants in the presence of different concentrations of NDGA.

bioRxiv preprint doi: https://doi.org/10.1101/2022.01.16.476523; this version posted January 17, 2022. The copyright holder for this preprint (which was not certified by peer review) is the author/funder, who has granted bioRxiv a license to display the preprint in perpetuity. It is made available under aCC-BY 4.0 International license.

662 Data shown in panel E are the mean ± SD. * indicates $P < 0.05$ and ** indicates $P <$

663 0.01 by Student's *t*-test.

664

bioRxiv preprint doi: https://doi.org/10.1101/2022.01.16.476523; this version posted January 17, 2022. The copyright holder for this preprint (which was not certified by peer review) is the author/funder, who has granted bioRxiv a license to display the preprint in perpetuity. It is made available under aCC-BY 4.0 International license.

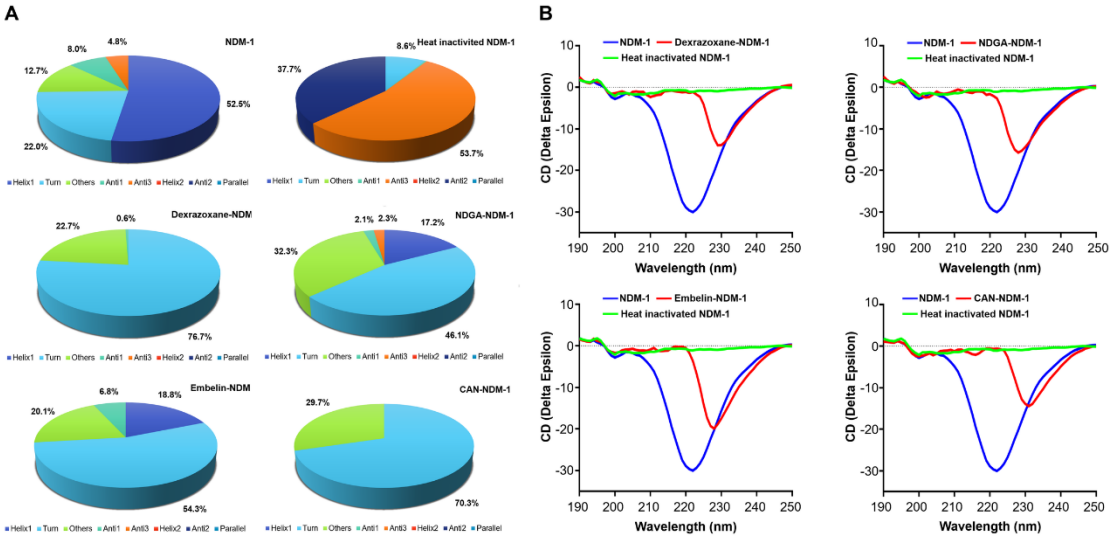

Figure 6. Inhibitors alter the secondary structure of NDM-1.

(**A**) Secondary structure composition of NDM-1 in the presence or absence of 32 µg/mL of the inhibitors as determined by CD spectra. **(B)** Calculated CD spectrum with dexrazoxane, NDGA, embelin and CAN on NDM-1. Comparison between NDM-1 (blue), NDM-1 treated with inhibitor (red) and heat inactivated NDM-1 (green) at 70 °C for 30 min. The wavelength for CD spectroscopy was set as 190-250 nm.

bioRxiv preprint doi: https://doi.org/10.1101/2022.01.16.476523; this version posted January 17, 2022. The copyright holder for this preprint (which was not certified by peer review) is the author/funder, who has granted bioRxiv a license to display the preprint in perpetuity. It is made available under aCC-BY 4.0 International license.

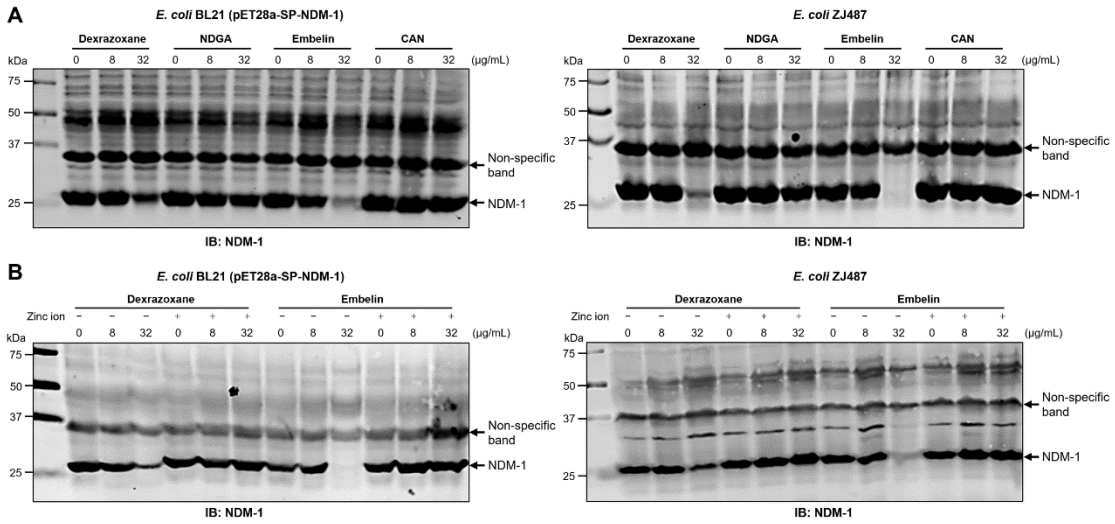

Figure 7. Dexrazoxane and embelin induce NDM-1 degradation via metal ion depletion manner.

(**A**) NDM-1 levels in *E. coli* strains BL21 (pET28a-SP-NDM-1) and ZJ487 treated with the indicated concentrations of inhibitors. (**B**) The addition of 500 μM of zinc ions suppresses the degradation of NDM-1 resulting from dexrazoxane and embelin treatment. Total proteins of bacteria cultured in the presence or absence of inhibitors and additional zinc ions were separated by SDS-PAGE and probed with NDM-1 specific antibody. The non-specific band was used as an internal loading control. The blots shown are one representative of three independent experiments with similar observations.

bioRxiv preprint doi: https://doi.org/10.1101/2022.01.16.476523; this version posted January 17, 2022. The copyright holder for this preprint (which was not certified by peer review) is the author/funder, who has granted bioRxiv a license to display the preprint in perpetuity. It is made available under aCC-BY 4.0 International license.

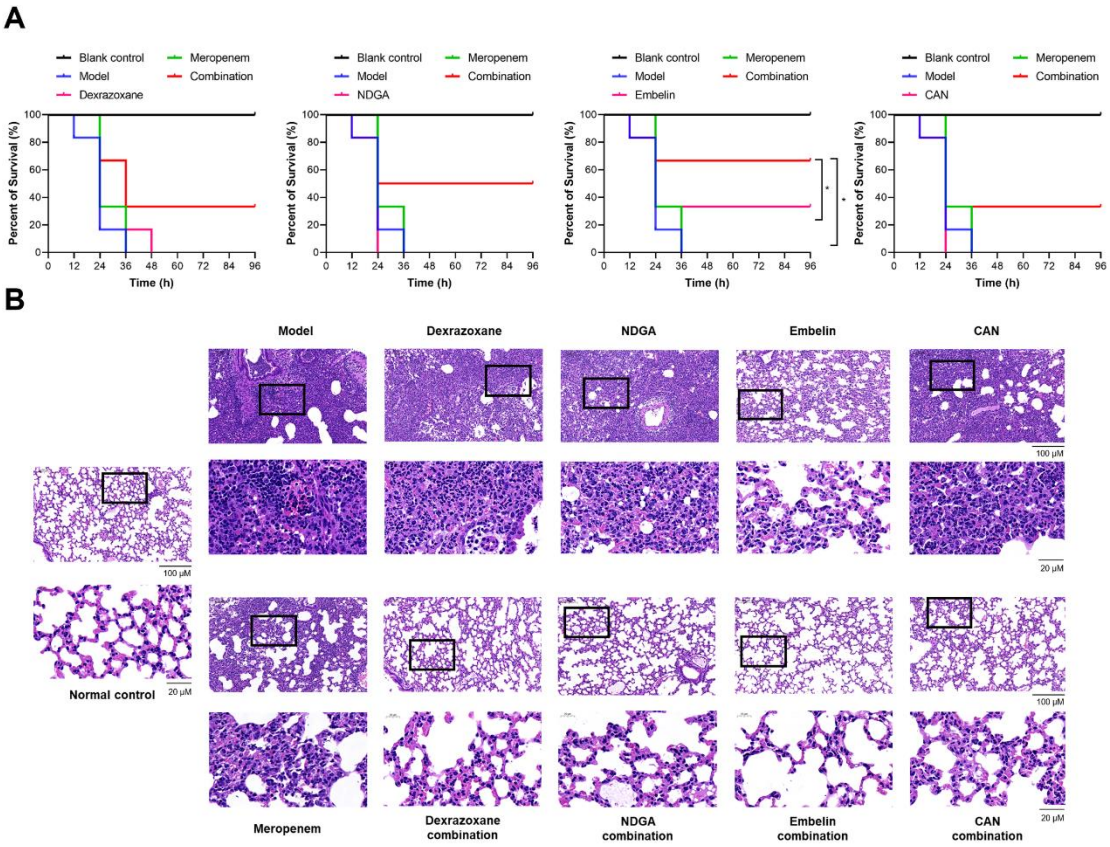

Figure 8. Dexrazoxane, NDGA, embelin and CAN rescue meropenem efficacy *in vivo*.

Mice were challenged with *E. coli* ZJ487 and then treated with inhibitors (80 mg/kg), meropenem (10 mg/kg), inhibitors (80 mg/kg) combined with meropenem (10 mg/kg) (combination), or DMSO (model). Mice without bacterial infection were included as a blank control. (**A**) The combination of individual inhibitors and meropenem significantly increased the survival rate of mice intraperitoneally infected with *E. coli* ZJ487 compared with meropenem monotherapy. Mice were randomly allocated into different groups and each group contained 6 mice (n=6). (**B**) The combination of individual inhibitors and meropenem alleviated histopathological injury of mice in a mouse pneumonia model compared with meropenem monotherapy. Lungs of infected mice were collected 72 h post-infection and stained with haematoxylin and eosin.

bioRxiv preprint doi: https://doi.org/10.1101/2022.01.16.476523; this version posted January 17, 2022. The copyright holder for this preprint (which was not certified by peer review) is the author/funder, who has granted bioRxiv a license to display the preprint in perpetuity. It is made available under aCC-BY 4.0 International license.

Histopathological changes were visualized under a digital slide scanner. Mice were randomly allocated into different groups and each group contained 6 mice (n=6). The experimental results shown in panels A and B are one representative from three independent experiments. * indicates $P < 0.05$ as determined by log-rank (Mantel-Cox) test.

bioRxiv preprint doi: https://doi.org/10.1101/2022.01.16.476523; this version posted January 17, 2022. The copyright holder for this preprint (which was not certified by peer review) is the author/funder, who has granted bioRxiv a license to display the preprint in perpetuity. It is made available under aCC-BY 4.0 International license.

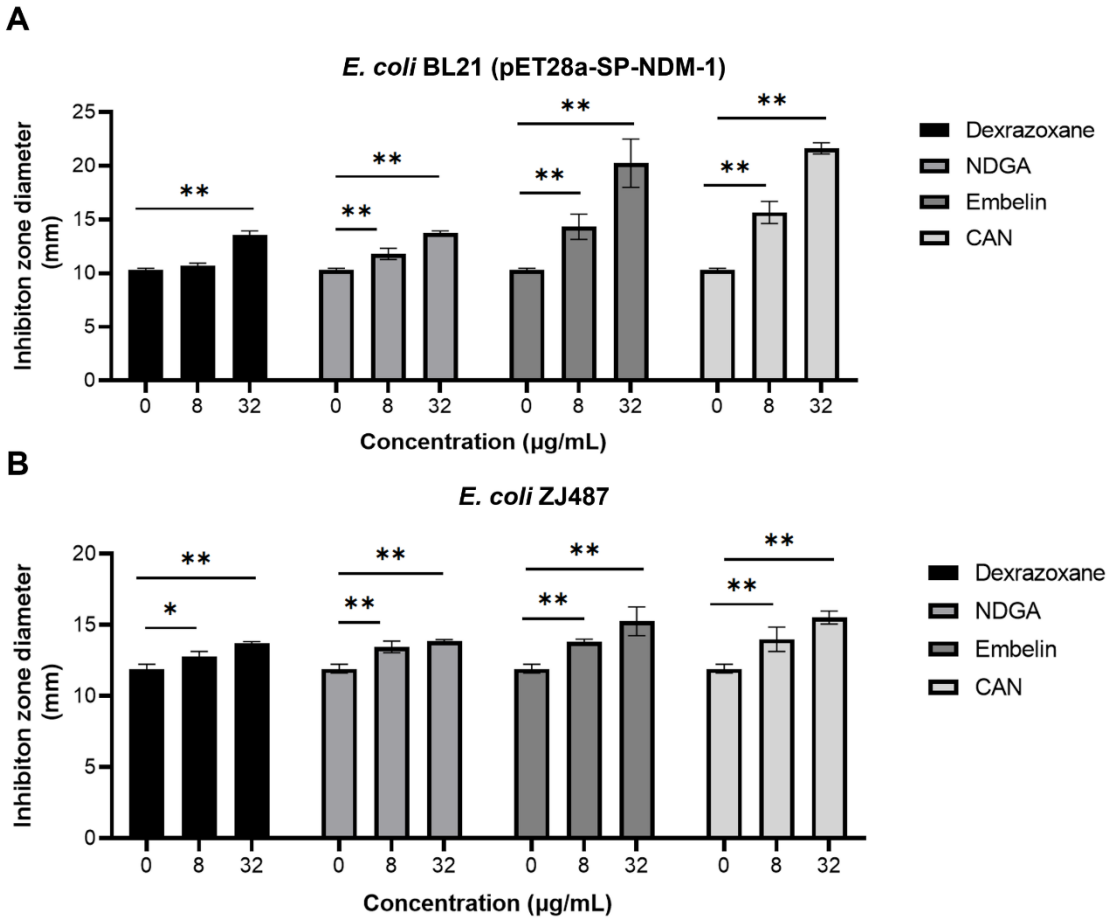

Figure 2- figure supplement 1. Dexrazoxane, NDGA, embelin and CAN rescued the activity of meropenem *in vitro* (related to Figure 2B).

The inhibition zone diameter of meropenem disks supplemented with 0 μg/mL, 8 μg/mL or 32 μg/mL of dexrazoxane, NDGA, embelin and CAN against *E. coli* strains BL21 (pET28a-SP-NDM-1) **(A)** and ZJ487 **(B)**. The data shown are the mean ± SD from three independent experiments. * indicates $P < 0.05$ and ** indicates $P < 0.01$ by Student's *t*-test.

bioRxiv preprint doi: https://doi.org/10.1101/2022.01.16.476523; this version posted January 17, 2022. The copyright holder for this preprint (which was not certified by peer review) is the author/funder, who has granted bioRxiv a license to display the preprint in perpetuity. It is made available under aCC-BY 4.0 International license.

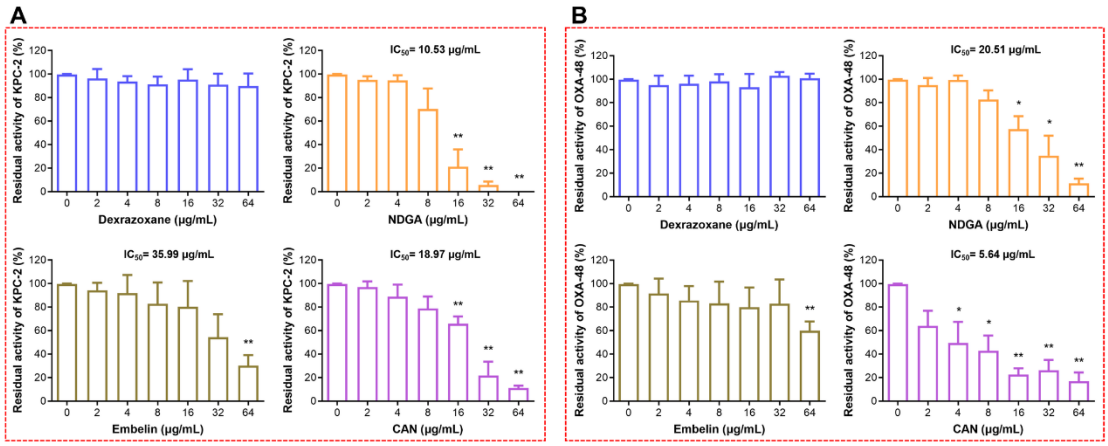

713

714 **Figure 3- figure supplement 1. Effects of dexrazoxane, NDGA, embelin and CAN**

715 **on the activity of KPC-2 and OXA-48.**

716 Inhibition of KPC-2 (**A**) and OXA-48 (**B**) by dexrazoxane, NDGA, embelin and CAN.

717 Data represent the mean ± SD from three independent experiments. * indicates $P < 0.05$

718 and ** indicates $P < 0.01$ by Student's *t*-test.

719

bioRxiv preprint doi: https://doi.org/10.1101/2022.01.16.476523; this version posted January 17, 2022. The copyright holder for this preprint (which was not certified by peer review) is the author/funder, who has granted bioRxiv a license to display the preprint in perpetuity. It is made available under aCC-BY 4.0 International license.

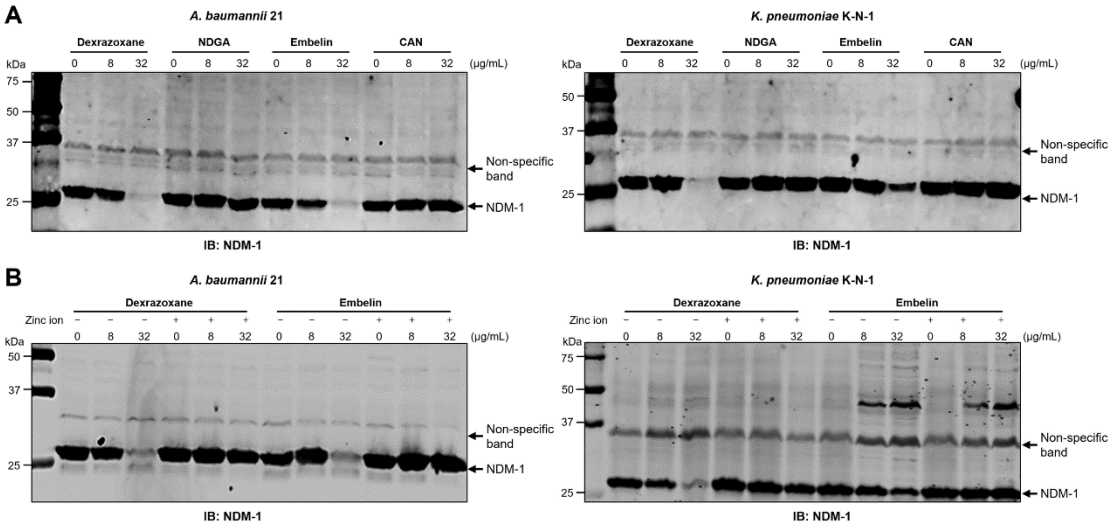

Figure 7- figure supplement 1. Dexrazoxane and embelin induce NDM-1 degradation via metal ion depletion manner.

(**A**) NDM-1 levels in *A. baumannii 21* and *K. pneumoniae* K-N-1 treated with the indicated concentrations of inhibitors. (**B**) The addition of 500 μM of zinc ions suppresses the degradation of NDM-1 resulting from dexrazoxane and embelin treatment. Total proteins of bacteria cultured in the presence or absence of inhibitors and additional zinc ions were separated by SDS-PAGE and probed with NDM-1 specific antibody. The non-specific band was used as an internal loading control. The blots shown are one representative of three independent experiments with similar observations.

bioRxiv preprint doi: https://doi.org/10.1101/2022.01.16.476523; this version posted January 17, 2022. The copyright holder for this preprint (which was not certified by peer review) is the author/funder, who has granted bioRxiv a license to display the preprint in perpetuity. It is made available under aCC-BY 4.0 International license.

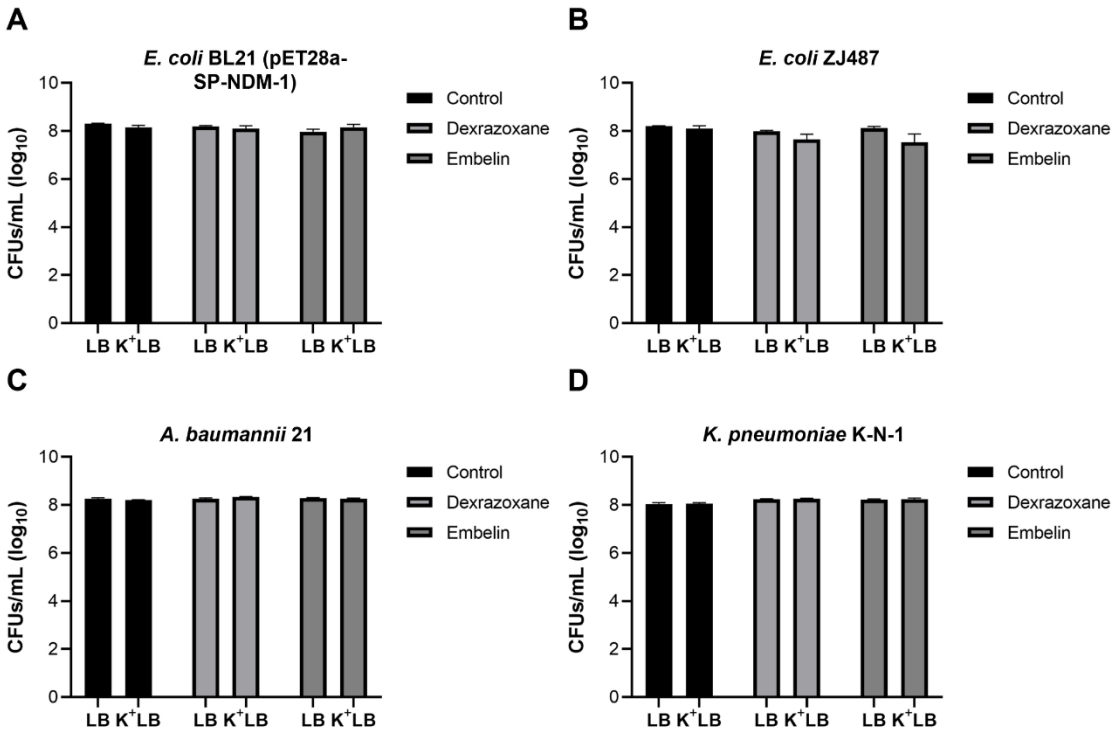

Figure 7- figure supplement 2. Dexrazoxane and embelin do not affect plasmid stability.

Plasmid stability of *E. coli* BL21 (pET28a-SP-NDM-1) (**A**), *E. coli* ZJ487 (**B**), *A. baumannii* 21 (**C**) or *K. pneumoniae* K-N-1 (**D**) following culture with 32 μg/mL of dexrazoxane or embelin. The data shown are the mean ± SD from three independent experiments.

bioRxiv preprint doi: https://doi.org/10.1101/2022.01.16.476523; this version posted January 17, 2022. The copyright holder for this preprint (which was not certified by peer review) is the author/funder, who has granted bioRxiv a license to display the preprint in perpetuity. It is made available under aCC-BY 4.0 International license.

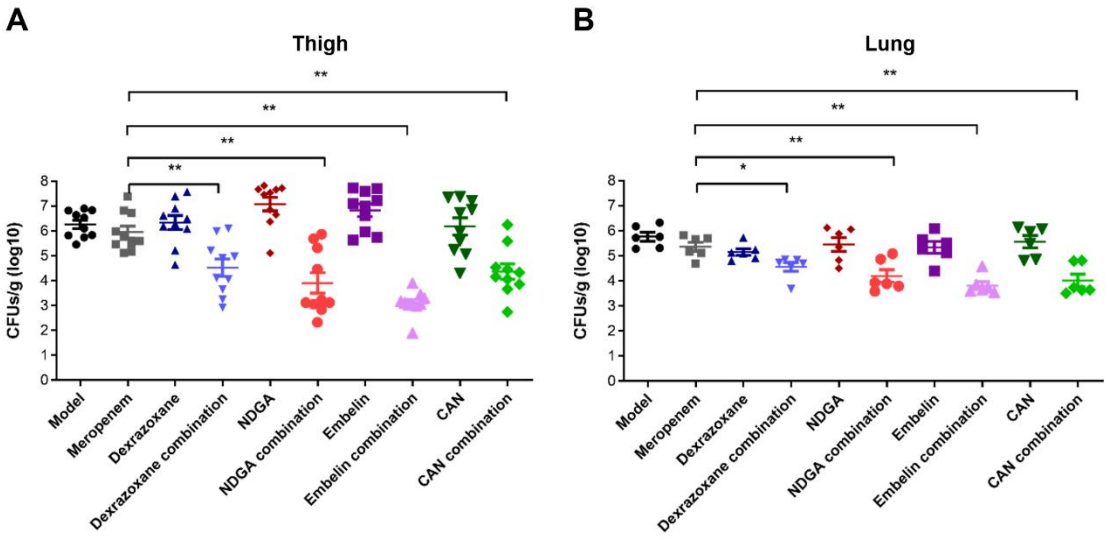

Figure 8- figure supplement 1. Dexrazoxane, NDGA, embelin and CAN rescue meropenem activity *in vivo*.

(**A**) The combination of meropenem with dexrazoxane, NDGA, embelin or CAN decreased the bacterial load in the mouse thigh infection model compared with the meropenem monotherapy. Mice were randomly allocated into different groups and each group contains 10 mice (n=10). (**B**) The combination of meropenem with dexrazoxane, NDGA, embelin or CAN reduced the bacterial load of the lungs in the mouse pneumonia model compared with the meropenem monotherapy (related to Figure 8B). Mice were randomly allocated into different groups and each group contains 6 mice (n=6). The data shown are one representative of three independent experiments. * indicates $P < 0.05$ and ** indicates $P < 0.01$ by Mann–Whitney U test.

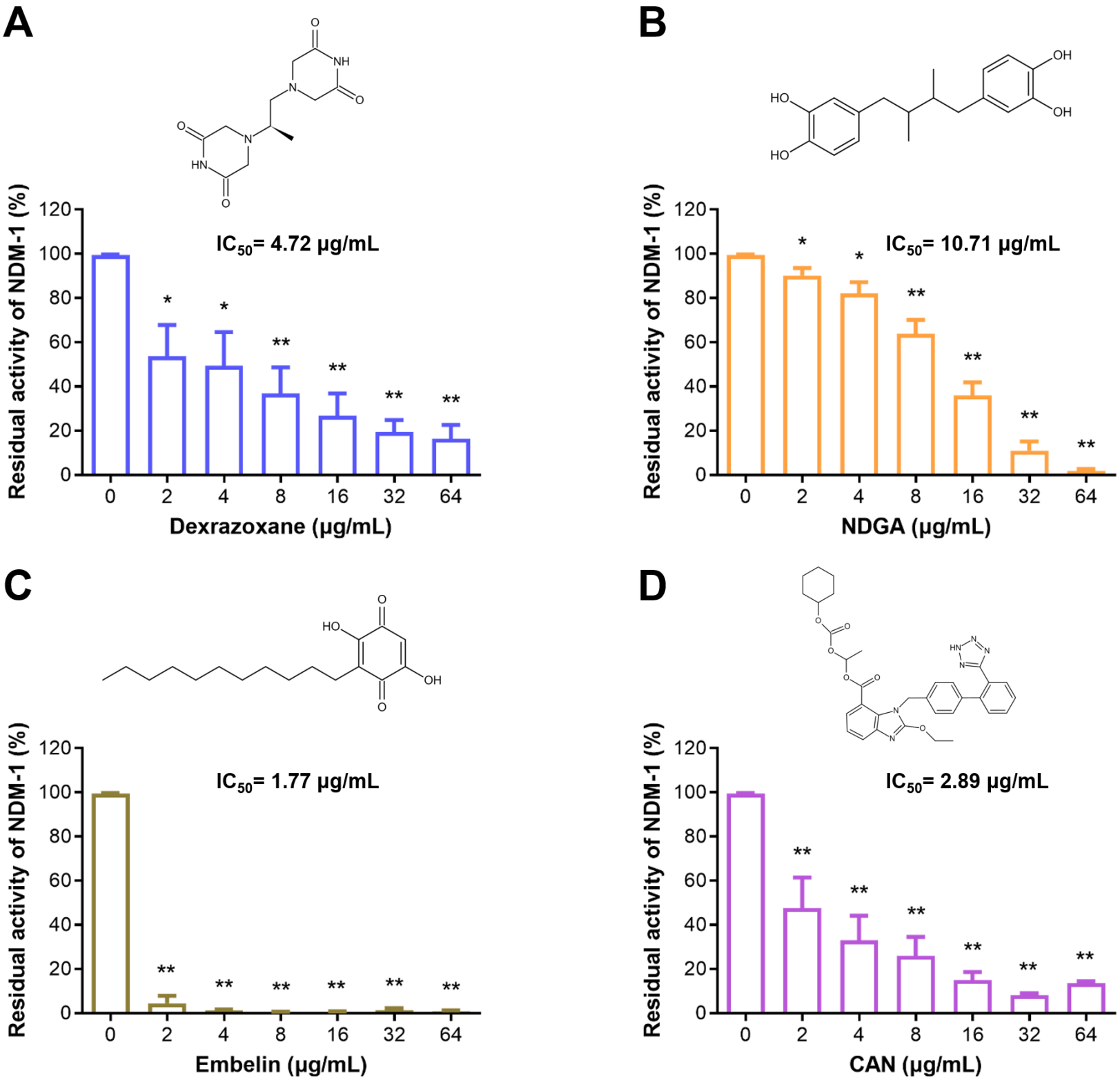
A
B
C
D
Residual activity of NDM-1 (%)
IC50= 4.72 μg/mL
Dexrazoxane (μg/mL)
IC50= 10.71 μg/mL
NDGA (μg/mL)
IC50= 1.77 μg/mL
Embelin (μg/mL)
IC50= 2.89 μg/mL
CAN (μg/mL)
0
2
4
8
16
32
64
20
40
60
80
100
120
*
**

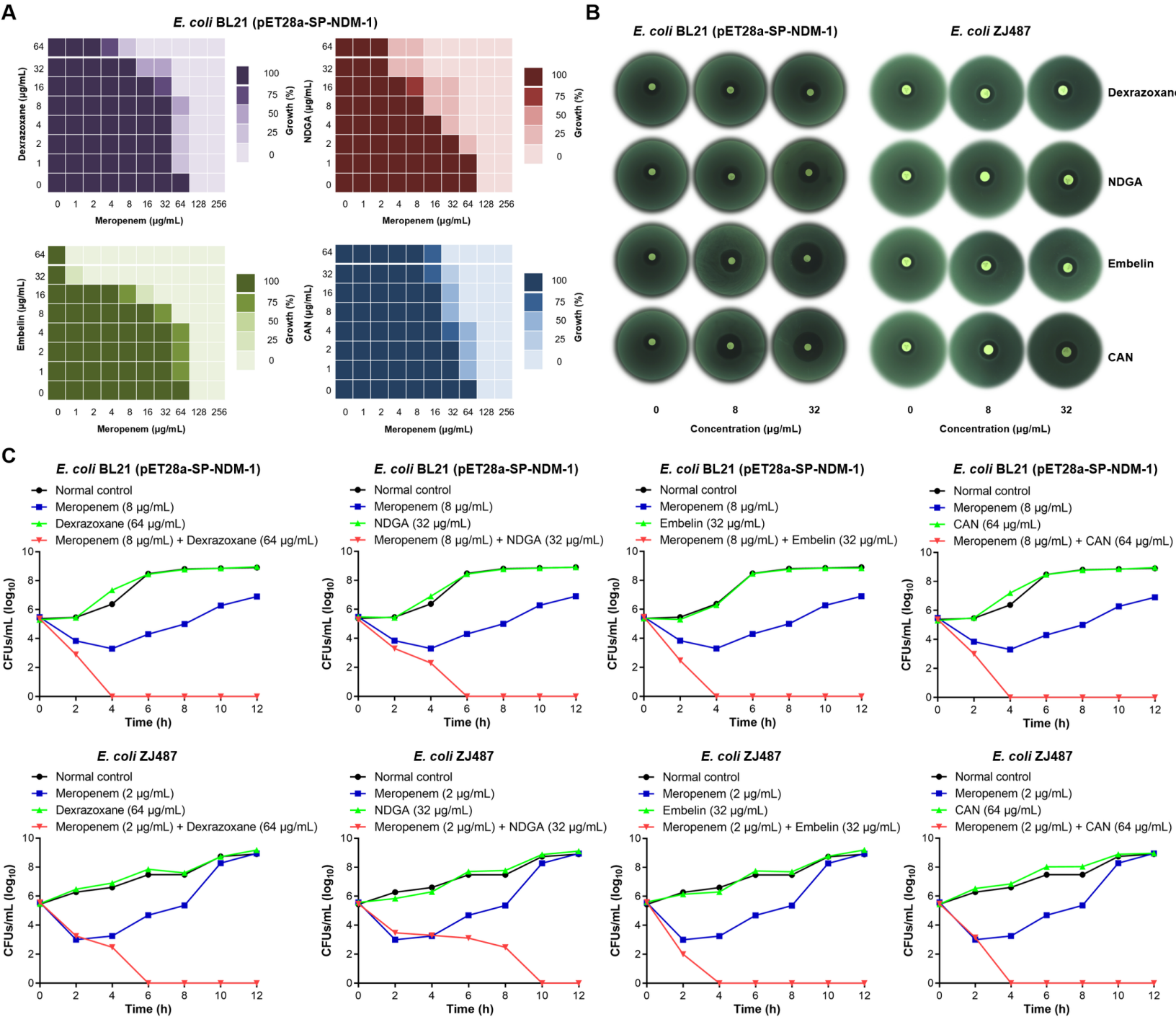
A
E. coli BL21 (pET28a-SP-NDM-1)
Dexrazoxane (μg/mL)
NDGA (μg/mL)
Embelin (μg/mL)
CAN (μg/mL)
Meropenem (μg/mL)
Growth (%)
B
E. coli BL21 (pET28a-SP-NDM-1)
E. coli ZJ487
Dexrazoxane
NDGA
Embelin
CAN
Concentration (μg/mL)
C
E. coli BL21 (pET28a-SP-NDM-1)
Normal control
Meropenem (8 μg/mL)
Dexrazoxane (64 μg/mL)
Meropenem (8 μg/mL) + Dexrazoxane (64 μg/mL)
NDGA (32 μg/mL)
Meropenem (8 μg/mL) + NDGA (32 μg/mL)
Embelin (32 μg/mL)
Meropenem (8 μg/mL) + Embelin (32 μg/mL)
CAN (64 μg/mL)
Meropenem (8 μg/mL) + CAN (64 μg/mL)
E. coli ZJ487
Meropenem (2 μg/mL)
Dexrazoxane (64 μg/mL)
Meropenem (2 μg/mL) + Dexrazoxane (64 μg/mL)
NDGA (32 μg/mL)
Meropenem (2 μg/mL) + NDGA (32 μg/mL)
Embelin (32 μg/mL)
Meropenem (2 μg/mL) + Embelin (32 μg/mL)
CAN (64 μg/mL)
Meropenem (2 μg/mL) + CAN (64 μg/mL)
CFUs/mL (log10)
Time (h)

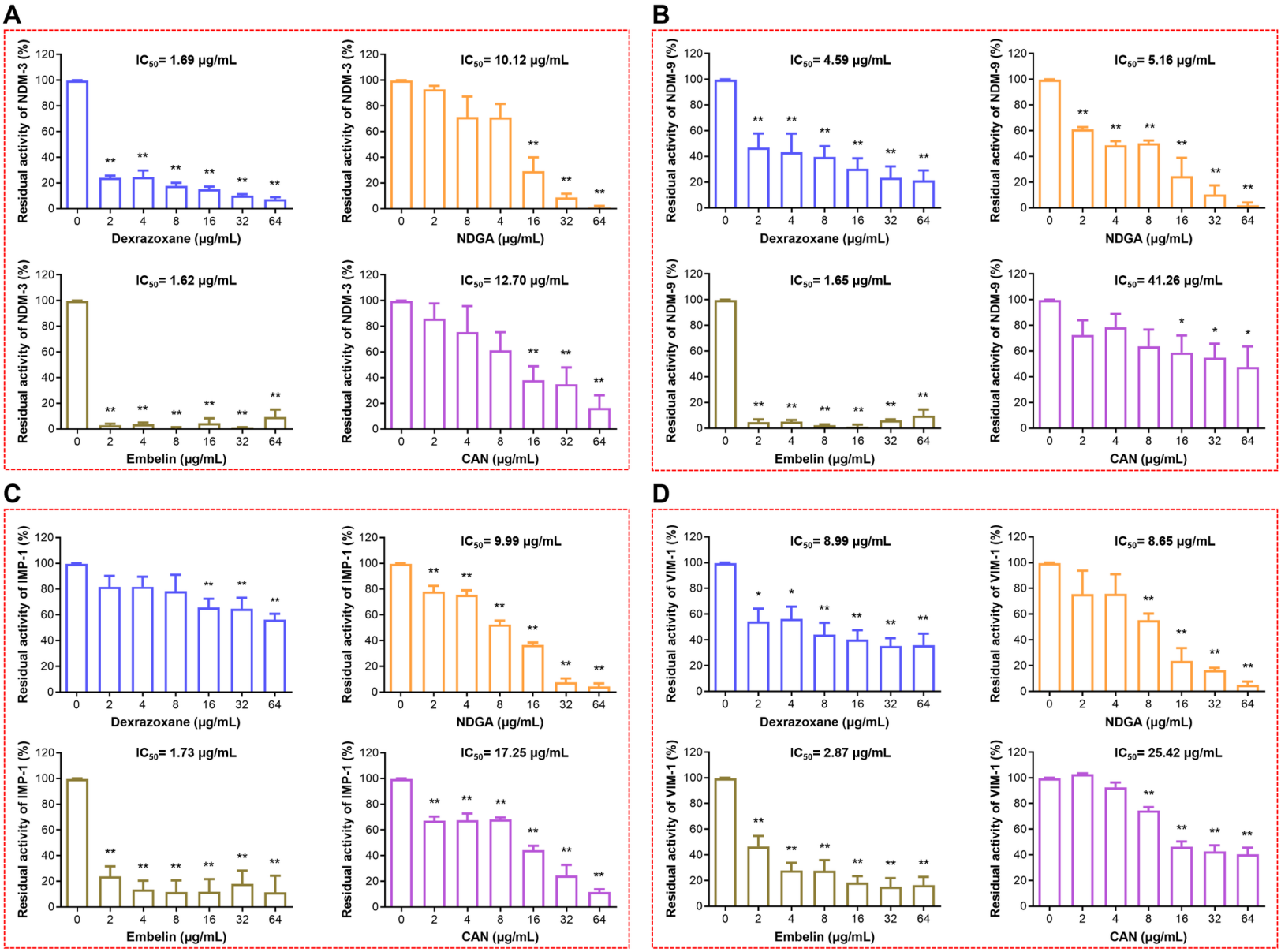
A
Residual activity of NDM-3 (%)
IC50= 1.69 μg/mL
Dexrazoxane (μg/mL)
IC50= 10.12 μg/mL
NDGA (μg/mL)
IC50= 1.62 μg/mL
Embelin (μg/mL)
IC50= 12.70 μg/mL
CAN (μg/mL)
B
Residual activity of NDM-9 (%)
IC50= 4.59 μg/mL
Dexrazoxane (μg/mL)
IC50= 5.16 μg/mL
NDGA (μg/mL)
IC50= 1.65 μg/mL
Embelin (μg/mL)
IC50= 41.26 μg/mL
CAN (μg/mL)
C
Residual activity of IMP-1 (%)
Dexrazoxane (μg/mL)
IC50= 9.99 μg/mL
NDGA (μg/mL)
IC50= 1.73 μg/mL
Embelin (μg/mL)
IC50= 17.25 μg/mL
CAN (μg/mL)
D
Residual activity of VIM-1 (%)
IC50= 8.99 μg/mL
Dexrazoxane (μg/mL)
IC50= 8.65 μg/mL
NDGA (μg/mL)
IC50= 2.87 μg/mL
Embelin (μg/mL)
IC50= 25.42 μg/mL
CAN (μg/mL)

Figure 4

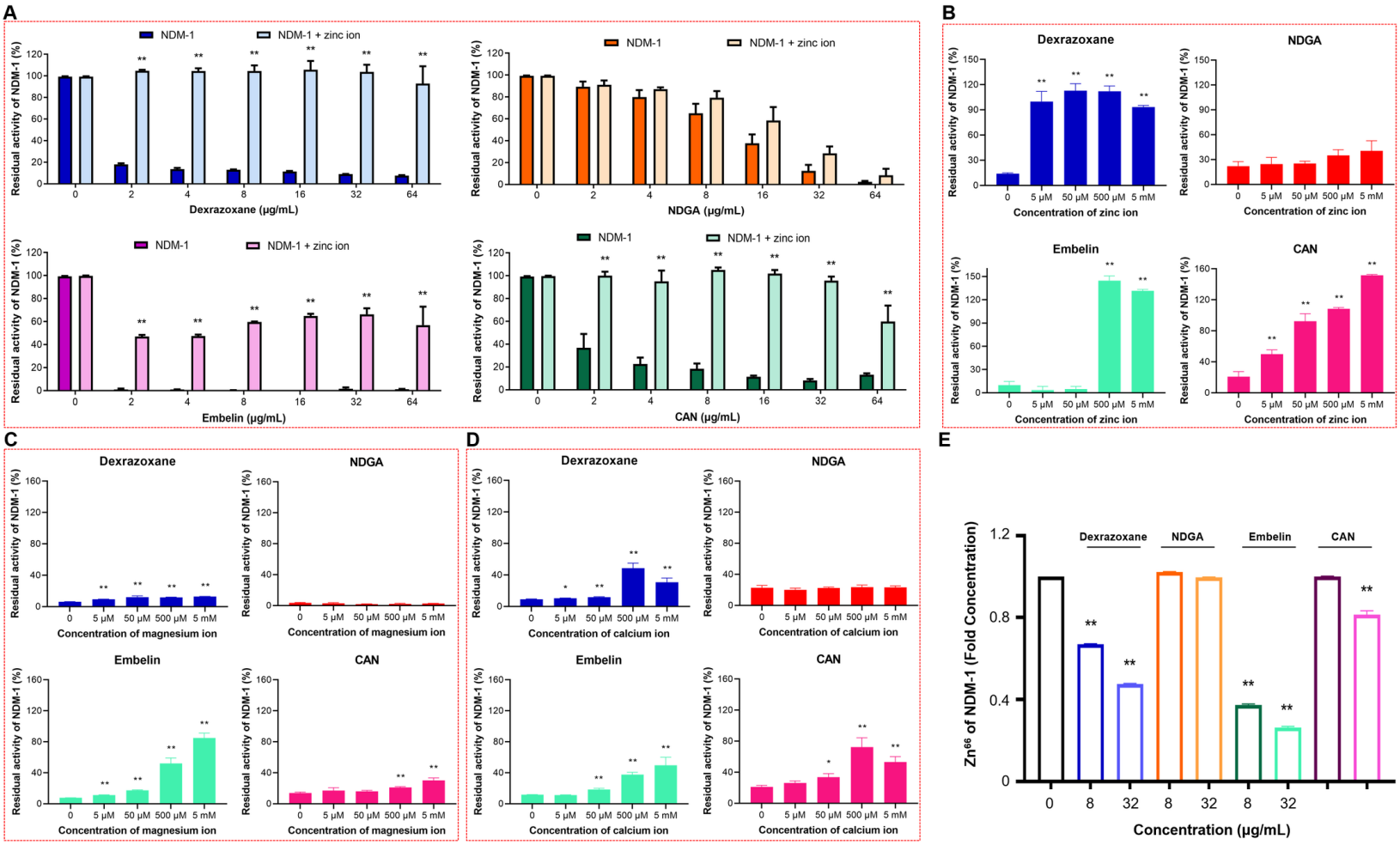
A
NDM-1
NDM-1 + zinc ion
Residual activity of NDM-1 (%)
Dexrazoxane (μg/mL)
NDGA (μg/mL)
Embelin (μg/mL)
CAN (μg/mL)
B
Dexrazoxane
NDGA
Embelin
CAN
Concentration of zinc ion
0
5 μM
50 μM
500 μM
5 mM
C
Concentration of magnesium ion
D
Concentration of calcium ion
E
Zn66 of NDM-1 (Fold Concentration)
Concentration (μg/mL)

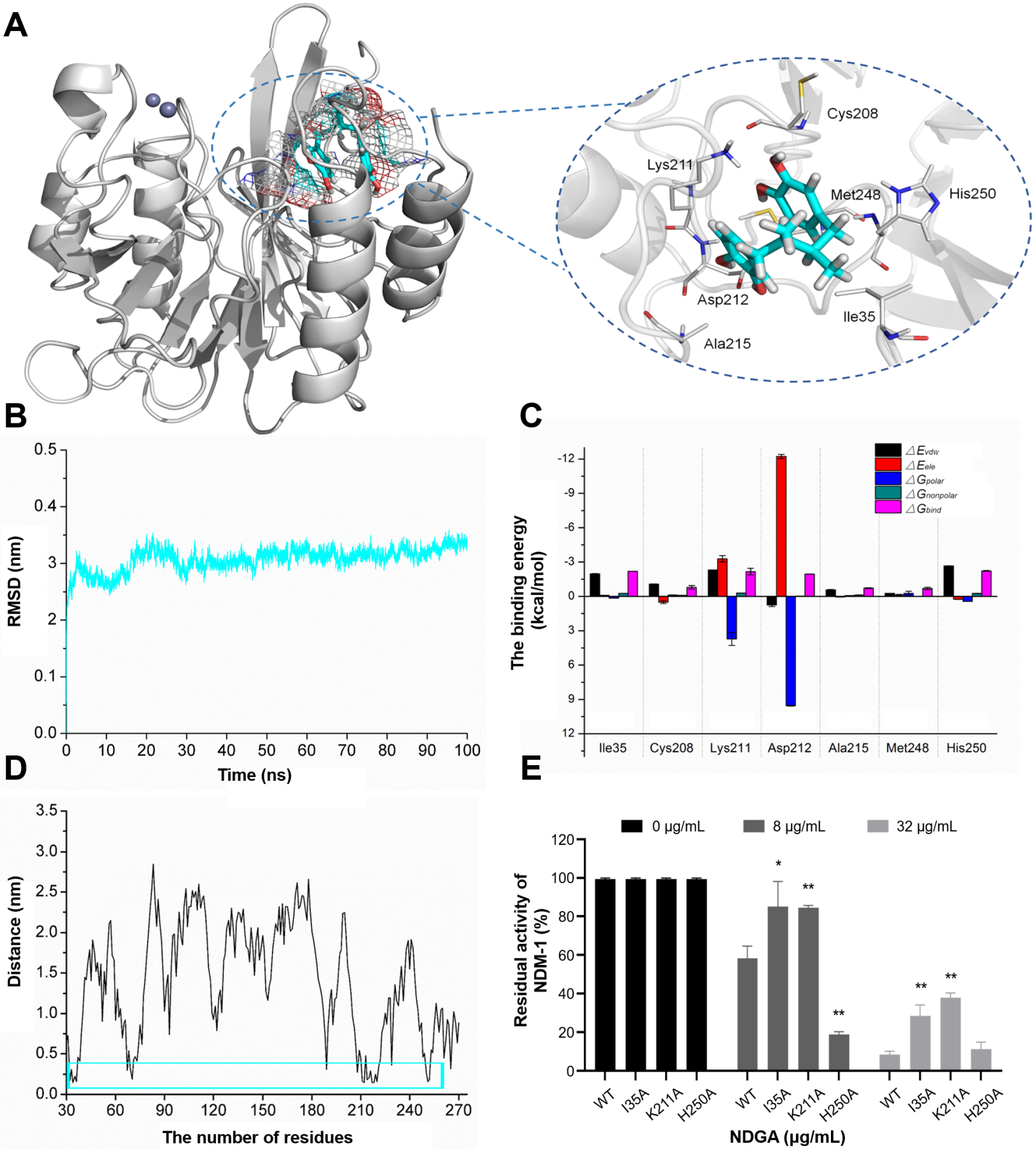
A
Cys208
Lys211
Met248
His250
Asp212
Ile35
Ala215
B
RMSD (nm)
Time (ns)
C
The binding energy (kcal/mol)
ΔEvdw
ΔEele
ΔGpolar
ΔGnonpolar
ΔGbind
Ile35
Cys208
Lys211
Asp212
Ala215
Met248
His250
D
Distance (nm)
The number of residues
E
0 μg/mL
8 μg/mL
32 μg/mL
Residual activity of NDM-1 (%)
WT
I35A
K211A
H250A
NDGA (μg/mL)

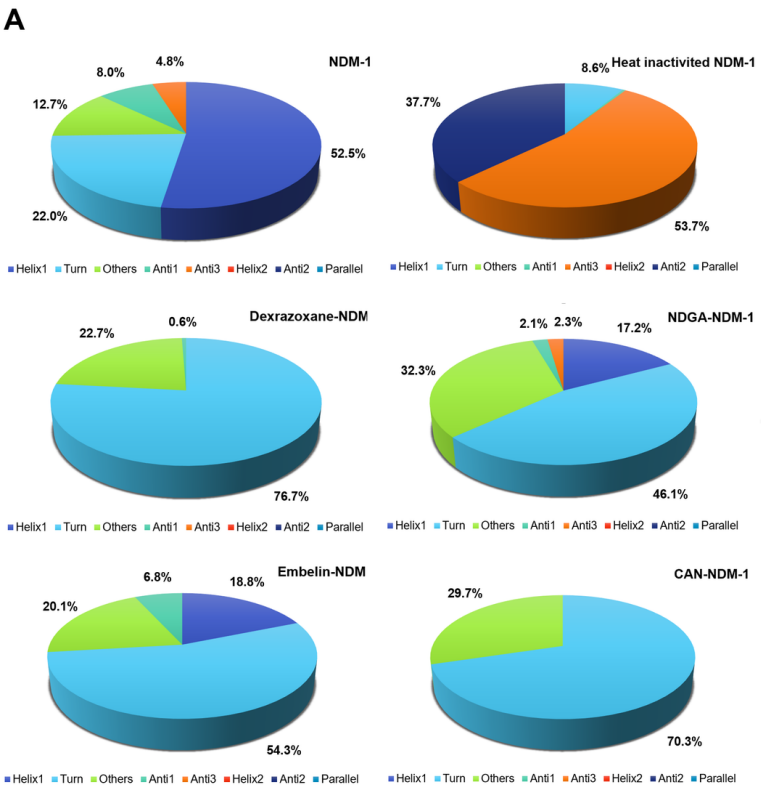
A
NDM-1
4.8%
8.0%
12.7%
52.5%
22.0%
Heat inactivited NDM-1
8.6%
37.7%
53.7%
Dexrazoxane-NDM
0.6%
22.7%
76.7%
NDGA-NDM-1
2.1%
2.3%
17.2%
32.3%
46.1%
Embelin-NDM
6.8%
18.8%
20.1%
54.3%
CAN-NDM-1
29.7%
70.3%
Helix1 Turn Others Anti1 Anti3 Helix2 Anti2 Parallel

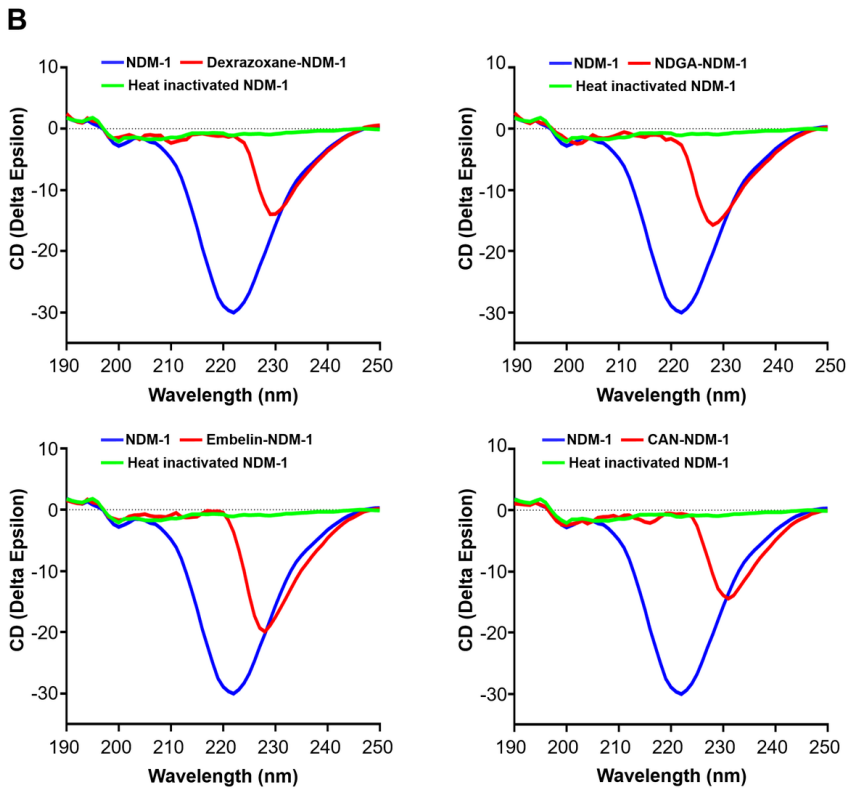
B
NDM-1
Dexrazoxane-NDM-1
Heat inactivated NDM-1
NDGA-NDM-1
Embelin-NDM-1
CAN-NDM-1
CD (Delta Epsilon)
Wavelength (nm)
10
0
-10
-20
-30
190 200 210 220 230 240 250

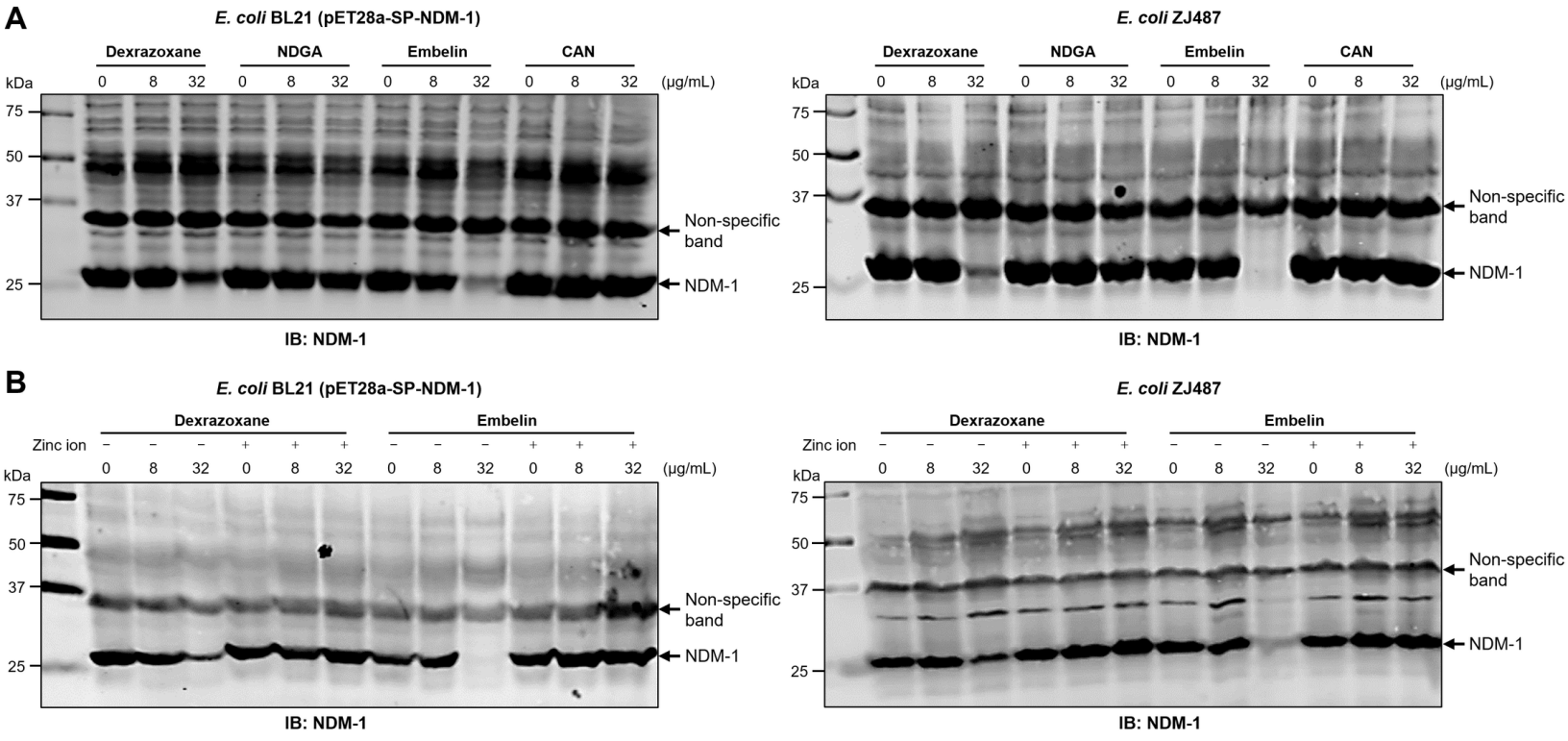
A
E. coli BL21 (pET28a-SP-NDM-1)
Dexrazoxane
NDGA
Embelin
CAN
kDa
0 8 32 0 8 32 0 8 32 0 8 32 (μg/mL)
75
50
37
25
Non-specific band
NDM-1
IB: NDM-1
E. coli ZJ487
Dexrazoxane
NDGA
Embelin
CAN
kDa
0 8 32 0 8 32 0 8 32 0 8 32 (μg/mL)
75
50
37
25
Non-specific band
NDM-1
IB: NDM-1
B
E. coli BL21 (pET28a-SP-NDM-1)
Dexrazoxane
Embelin
Zinc ion
– – – + + + – – – + + +
kDa
0 8 32 0 8 32 0 8 32 0 8 32 (μg/mL)
75
50
37
25
Non-specific band
NDM-1
IB: NDM-1
E. coli ZJ487
Dexrazoxane
Embelin
Zinc ion
– – – + + + – – – + + +
kDa
0 8 32 0 8 32 0 8 32 0 8 32 (μg/mL)
75
50
37
25
Non-specific band
NDM-1
IB: NDM-1

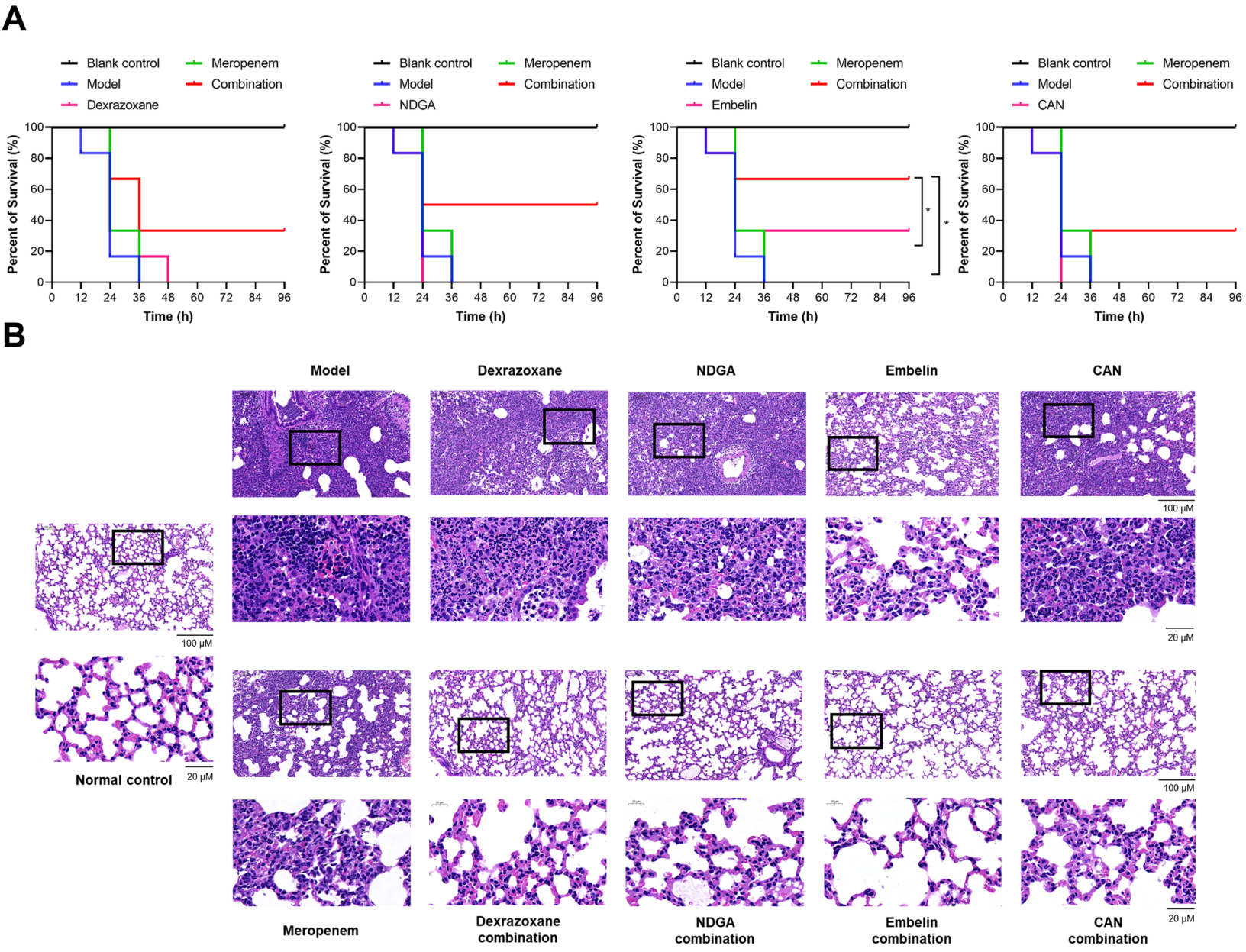
A
Blank control
Model
Dexrazoxane
Meropenem
Combination
NDGA
Embelin
CAN
Percent of Survival (%)
Time (h)
0
12
24
36
48
60
72
84
96
20
40
80
100
*
B
Model
Dexrazoxane
NDGA
Embelin
CAN
Normal control
Meropenem
Dexrazoxane combination
NDGA combination
Embelin combination
CAN combination
100 μM
20 μM

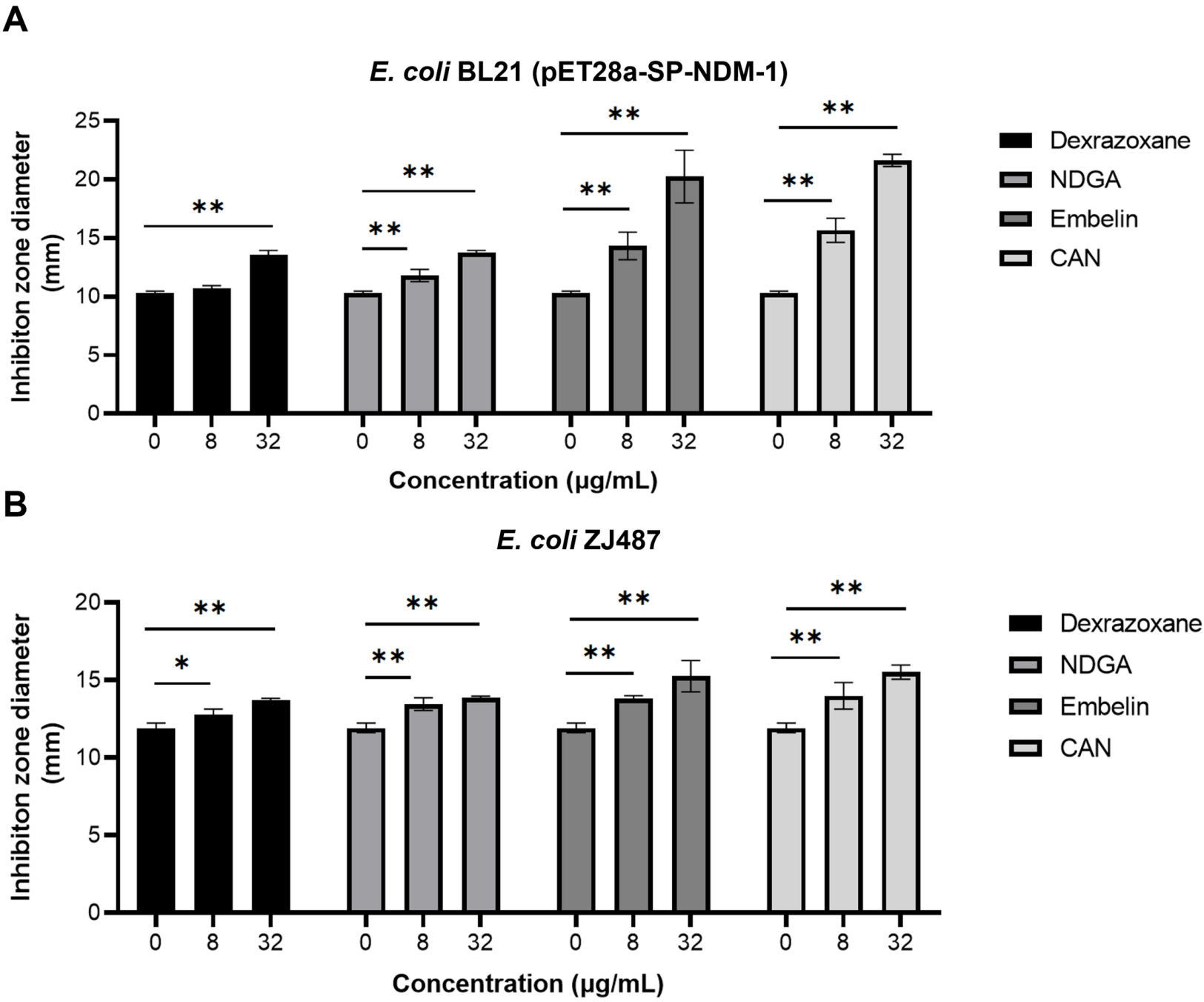
A
E. coli BL21 (pET28a-SP-NDM-1)
Inhibiton zone diameter (mm)
25
20
15
10
5
0
**
**
**
**
**
**
**
**
0
8
32
0
8
32
0
8
32
0
8
32
Concentration (μg/mL)
Dexrazoxane
NDGA
Embelin
CAN
B
E. coli ZJ487
Inhibiton zone diameter (mm)
20
15
10
5
0
*
**
**
**
**
**
**
**
0
8
32
0
8
32
0
8
32
0
8
32
Concentration (μg/mL)
Dexrazoxane
NDGA
Embelin
CAN

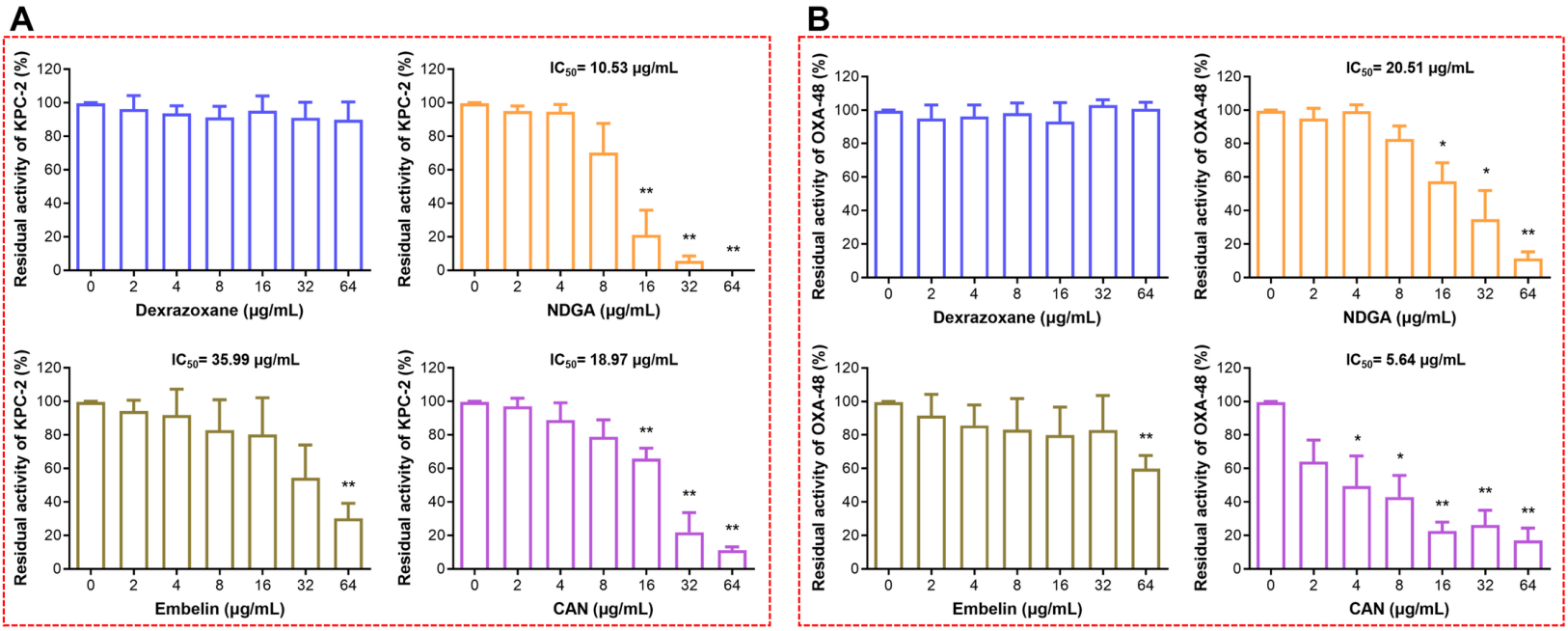
A
B
Residual activity of KPC-2 (%)
Residual activity of OXA-48 (%)
Dexrazoxane (μg/mL)
NDGA (μg/mL)
Embelin (μg/mL)
CAN (μg/mL)
IC50= 10.53 μg/mL
IC50= 20.51 μg/mL
IC50= 35.99 μg/mL
IC50= 18.97 μg/mL
IC50= 5.64 μg/mL
0 2 4 8 16 32 64
0 20 40 60 80 100 120
* **

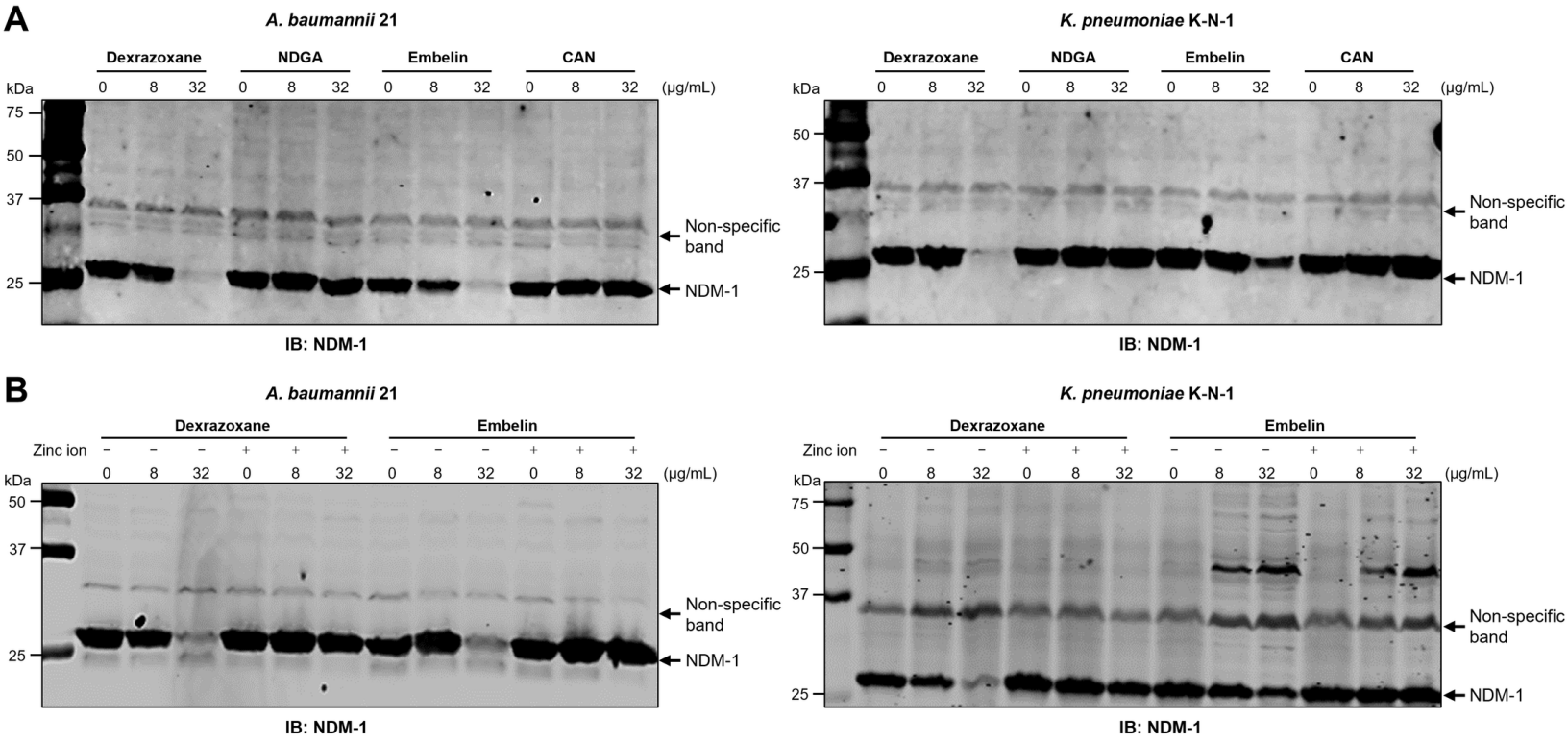
A
A. baumannii 21
Dexrazoxane
NDGA
Embelin
CAN
kDa
0 8 32 0 8 32 0 8 32 0 8 32 (μg/mL)
75
50
37
25
Non-specific band
NDM-1
IB: NDM-1
K. pneumoniae K-N-1
Dexrazoxane
NDGA
Embelin
CAN
kDa
0 8 32 0 8 32 0 8 32 0 8 32 (μg/mL)
50
37
25
Non-specific band
NDM-1
IB: NDM-1
B
A. baumannii 21
Dexrazoxane
Embelin
Zinc ion
– – – + + +
kDa
0 8 32 0 8 32 0 8 32 0 8 32 (μg/mL)
50
37
25
Non-specific band
NDM-1
IB: NDM-1
K. pneumoniae K-N-1
Dexrazoxane
Embelin
Zinc ion
– – – + + +
kDa
0 8 32 0 8 32 0 8 32 0 8 32 (μg/mL)
75
50
37
25
Non-specific band
NDM-1
IB: NDM-1

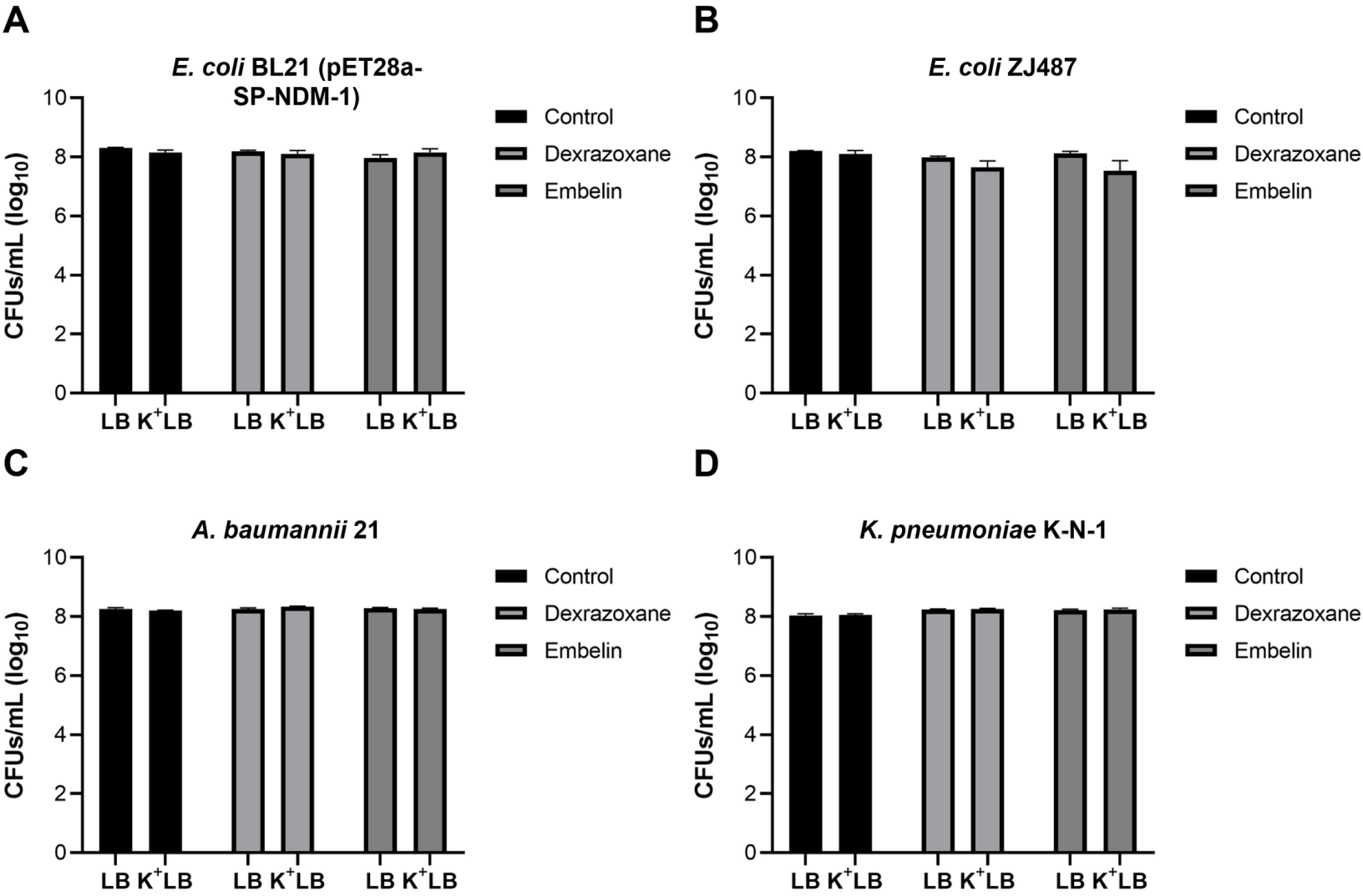
A
E. coli BL21 (pET28a-SP-NDM-1)
B
E. coli ZJ487
C
A. baumannii 21
D
K. pneumoniae K-N-1
CFUs/mL (log10)
0
2
4
6
8
10
LB
K+LB
Control
Dexrazoxane
Embelin

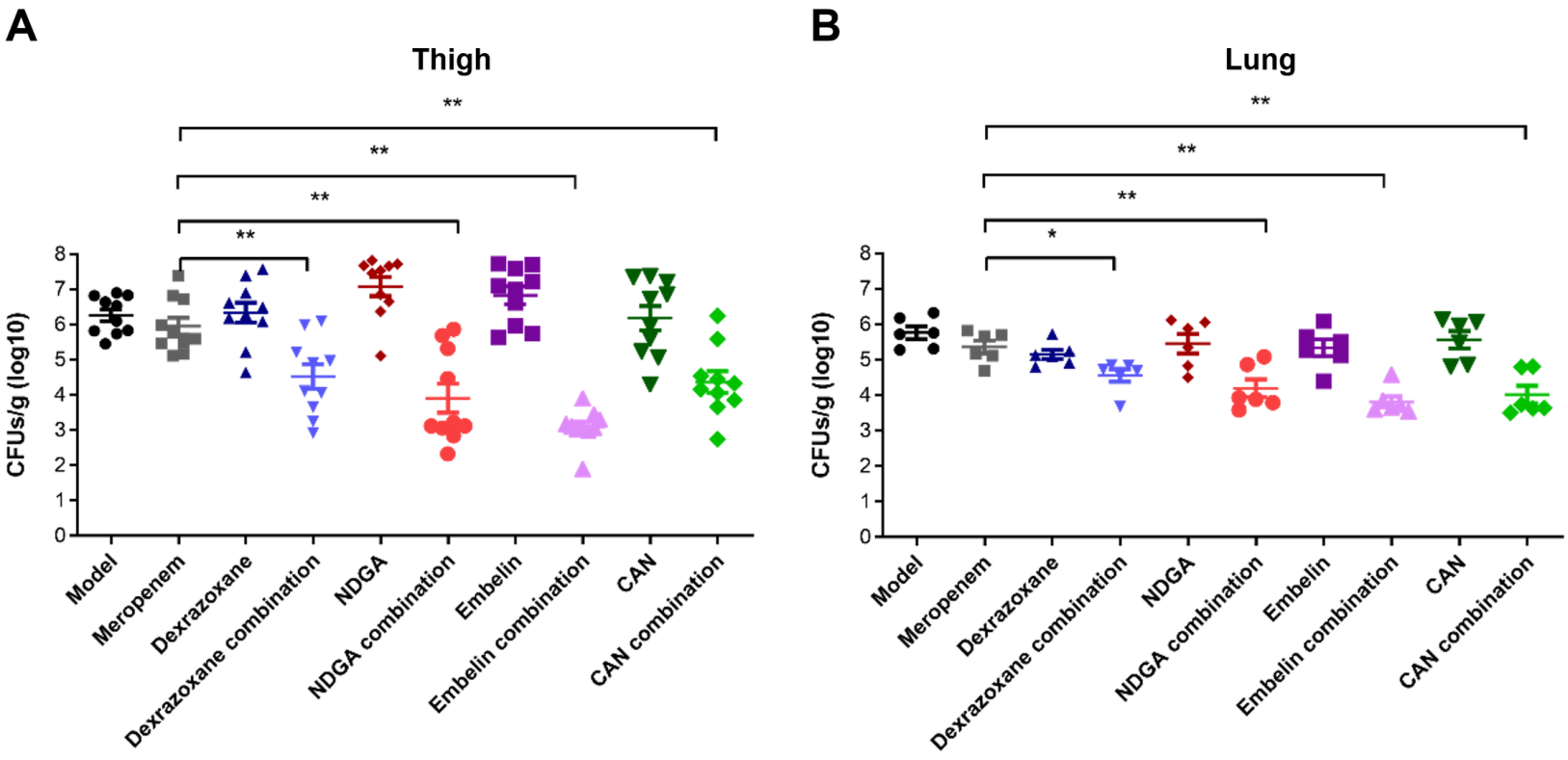
A
Thigh
B
Lung
CFUs/g (log10)
0
1
2
3
4
5
6
7
8
*
**
Model
Meropenem
Dexrazoxane
Dexrazoxane combination
NDGA
NDGA combination
Embelin
Embelin combination
CAN
CAN combination